JBC RESEARCH ARTICLE

Deciphering the interaction between PKM2 and the built-in thermodynamic properties of the glycolytic pathway in cancer cells

Received for publication, January 12, 2024, and in revised form, March 24, 2024 Published, Papers in Press, August 8, 2024,
https://doi.org/10.1016/j.jbc.2024.107648

Chengmeng Jin[1,2,3,4], **Wei Hu**[5], **Yuqi Wang**[1], **Hao Wu**[1,2,3,4], **Siying Zeng**[1], **Minfeng Ying**[1,2,3,4], and **Xun Hu**[1,2,3,4,*]

From the [1]*Cancer Institute (Key Laboratory of Cancer Prevention and Intervention, China National Ministry of Education), The Second Affiliated Hospital, Zhejiang University School of Medicine, Hangzhou, Zhejiang, China;* [2]*Zhejiang Province Key Laboratory of Molecular Biology in Medical Sciences, Hangzhou, Zhejiang, China;* [3]*Zhejiang Provincial Clinical Research Center for Cancer, Hangzhou, Zhejiang, China;* [4]*Cancer Center of Zhejiang University, Hangzhou, Zhejiang, China;* [5]*Center for Nutrition & Food Sciences, Queensland Alliance for Agriculture and Food Innovation, The University of Queensland, Saint Lucia, QLD, Australia*

Reviewed by members of the JBC Editorial Board. Edited by Alex Toker

Most cancer cells exhibit high glycolysis rates under conditions of abundant oxygen. Maintaining a stable glycolytic rate is critical for cancer cell growth as it ensures sufficient conversion of glucose carbons to energy, biosynthesis, and redox balance. Here we deciphered the interaction between PKM2 and the thermodynamic properties of the glycolytic pathway. Knocking down or knocking out PKM2 induced a thermodynamic equilibration in the glycolytic pathway, characterized by the reciprocal changes of the Gibbs free energy (ΔG) of the reactions catalyzed by PFK1 and PK, leading to a less exergonic PFK1-catalyzed reaction and a more exergonic PK-catalyzed reaction. The changes in the ΔGs of the two reactions cause the accumulation of intermediates, including the substrate PEP (the substrate of PK), in the segment between PFK1 and PK. The increased concentration of PEP in turn increased PK activity in the glycolytic pathway. Thus, the interaction between PKM2 and the thermodynamic properties of the glycolytic pathway maintains the reciprocal relationship between PK concentration and its substrate PEP concentration, by which, PK activity in the glycolytic pathway can be stabilized and effectively counteracts the effect of PKM2 KD or KO on glycolytic rate. In line with our previous reports, this study further validates the roles of the thermodynamics of the glycolytic pathway in stabilizing glycolysis in cancer cells. Deciphering the interaction between glycolytic enzymes and the thermodynamics of the glycolytic pathway will promote a better understanding of the flux control of glycolysis in cancer cells.

Warburg effect is a metabolic hallmark of rapidly proliferating cancer cells, characterized by high glycolysis rates even under ample oxygen (1). The glycolytic rate in cancer cells is much higher than that in normal differentiated cells (2, 3). The high rate of glycolysis has three major metabolic purposes to support the rapid growth of cancer cells (4). Firstly, the fast degradation of glucose transfers the energy to produce ATP. Secondly, the intermediates in the glycolysis flux shuttle to metabolic branches subsidiary to glycolysis for biosynthesis, for example, G6P is used to generate NADPH and ribose-5-phosphate through pentose phosphate pathway, DHAP is used to generate glycerol 3-phosphate, 3-PG is used to generate serine *via* serine synthesis pathway, and among others. Finally, NADPH generated from the oxidative branch of the pentose phosphate pathway is the major reducing power not only for supporting biosynthesis but also for maintaining redox homeostasis.

Hence, a stably high rate of glycolysis is important for supporting the rapid proliferation of cancer cells. Maintaining such a stable rate depends on two factors. The first factor is the glycolytic enzymes, whose activities should be sufficiently high to keep the rate. In cancer cells, glycolytic enzymes are overexpressed (4, 5). The second factor is the thermodynamic properties of the glycolytic pathways, but its role in the flux control of glycolysis is not well understood. We hypothesize that the glycolytic enzymes and thermodynamic properties in the glycolytic pathway tightly coordinate with each other and through this coordination, the glycolytic rate may be stabilized even when individual glycolytic enzymes are perturbed. We used PKM2 knockdown as a model to test this hypothesis. The rationale for choosing PKM2 as a model is based on the following: firstly, the activity of PKM2 in cancer cells is highly sensitive to regulations, including expression, allosteric regulation, posttranslational modification, oxidation (6–17); secondly, PKM2 is considered as the last rate-limiting enzyme in the glycolysis (6–9), as it catalyzes a highly exogonic reaction; thirdly, according to previous reports, PKM2 inhibition may lead to two possible consequences: glycolytic rate is sensitive (6–17) or resistant (18–20) to PKM2 perturbation, but the underlying mechanisms are not provided.

Despite the remarkable progress in understanding the role of PKM2 in glycolysis, we noticed that the thermodynamics of the glycolytic pathway were not taken into consideration in previous studies. In theory, rate control is an issue of both

* For correspondence: Xun Hu, huxun@zju.edu.cn.

kinetics and thermodynamics. Recently, we found that when the glycolytic enzyme GAPDH is knocked down or inhibited by iodoacetate (a GAPDH inhibitor), it induces concentration changes in the glycolytic intermediates, which are controlled by the built-in thermodynamic properties of the glycolytic pathway (ΔGs of the reactions along the glycolytic pathway) (21). The thermodynamic properties allow an automatic regulation of the concentration of GA3P (the substrate of GAPDH) and the concentration of GAPDH: As GAPDH concentration decreases, GA3P concentration increases, and *vice versa*. Knocking down another glycolytic enzyme, PGK1, yielded the same results (22). These studies reveal the role of thermodynamics of the glycolytic pathway in stabilizing the rate of glycolysis. By analogy, the thermodynamic properties of the glycolytic pathway may also stabilize the rate of PKM2 in the glycolytic pathway. However, PKM2 is different from GAPDH and PGK1 in two aspects: The reactions catalyzed by GAPDH and PGK1 in the glycolysis pathway are at near-equilibrium states, whereas PKM2 catalyzes a highly exergonic reaction ($\Delta G < -20$ kJ/mol), far from equilibrium (21, 22); Secondly, PKM2 is regulated by multiple intracellular allosteric regulators. If thermodynamic properties in the glycolysis pathway could stabilize the rate of this critical step of glycolysis, it would further highlight its role in glycolysis.

Results

No or marginally significant effects of PKM2 KD or KO on glycolytic rate

The first question addressed in this study is whether PKM2 knockdown would significantly affect the steady-state rate of glycolysis. To investigate this, PKM2 in HeLa was knocked down by 80% (Fig. 1*A*), resulting in a 70% decrease in total PK activity (Fig. 1*A*). This difference is anticipated because, in

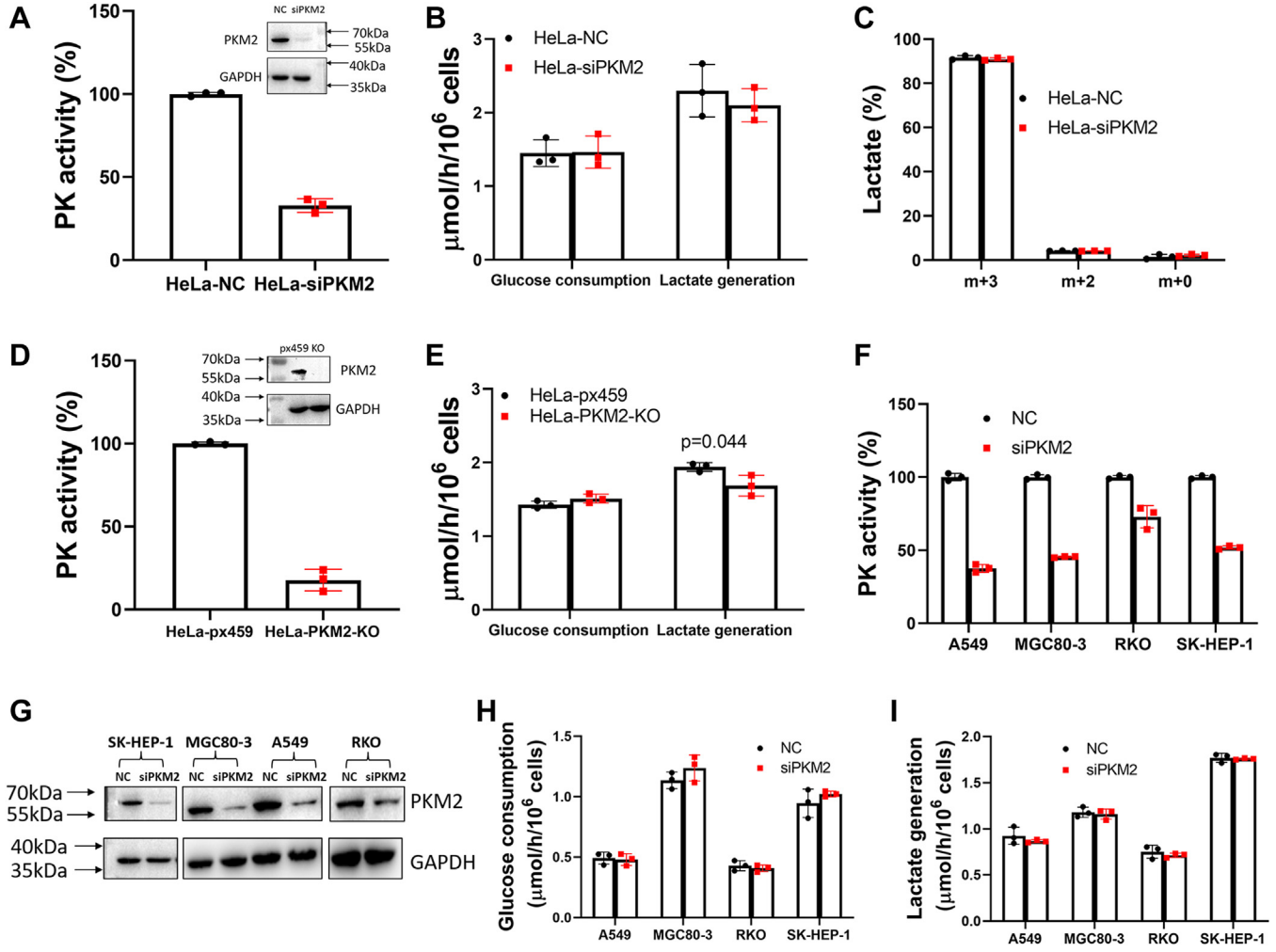

Figure 1. PKM2 KD or KO does not significantly affect the glycolytic rate in cancer cells. *A*, Western blot of PKM2 and enzyme activity of PK of HeLa-NC and HeLa-siPKM2 cells. *B*, glucose consumption rate and lactate generation rate of HeLa-NC and HeLa-siPKM2 cells. Cells were cultured in a complete RPMI-1640 medium for 4 h, then glucose concentration and lactate concentration in the culture medium were measured and the rates were calculated. *C*, tracing glucose carbon to lactate. After 48 h after siRNA transfection, HeLa-NC cells and HeLa-siPKM2 cells were incubated with 6 mM [$^{13}C_6$]glucose for 9 h, the medium was collected and the percentages of generated lactate isotopologues were measured by LC-MS as described in Materials and Method under the subheading of "Isotopic lactate determination by LC-MS/MS". *D*, Western blot of PKM2 and enzyme activity of PK of HeLa-px459 and HeLa-PKM2-KO cells. *E*, glucose consumption rate and lactate generation rate of HeLa-px459 and HeLa-PKM2-KO cells. *F*, PK activities of four cancer cell lines with or without PKM2 KD. *G*, Western blot of PKM2 of four cancer cell lines with or without PKM2 KD. *H* and *I*, glucose consumption rate and lactate generation rate of control and PKM2 KD cells. Data represent the mean ± SD of three independent experiments with each experiment performed in triplicates.

addition to PKM2, HeLa cells also contain other PK isoforms. The glycolytic rate (glucose consumption and lactate production) of HeLa-siPKM2 was not significantly different from that of HeLa-NC (Fig. 1*B*). There may be two reasons for this. The first reason is that after PKM2 is knocked down, the expression of other glycolytic enzymes in cells may be increased, which offsets the knockdown of PKM2. This possibility was ruled out because the activities of other glycolytic enzymes of HeLa-siPKM2 were not significantly different from those of HeLa-NC (Table S1). The second reason is that some lactate may be derived from other metabolic pathways, which masked PKM2-KD-induced decrease of glycolytic rate. By means of [$^{13}C_6$]-glucose tracing, we observed that the percentage of m3-lactate produced by HeLa-NC and HeLa-siPKM2 was not significantly different (Fig. 1*C*). Thus, the results support that PKM2 KD did not significantly affect the glycolytic rate in HeLa cells.

We are curious if the residual PK activity in PKM2 KO cells could maintain steady-state rate of glycolysis. We then knocked out PKM2 in HeLa cells. In HeLa-PKM2-KO cells, PKM2 was not detected (Fig. 1*D*), but 18% residual PK activity remained (Fig. 1*D*). Glucose consumption was not significantly altered in HeLa-PKM2 KO cells compared to control, and lactate production was only reduced by about 10% (Fig. 1*E*). The results demonstrated that even in the absence of PKM2, the residual PK activity can still maintain the glycolytic rate.

To verify that the results based on HeLa cells are not a special case, we knocked down PKM2 in four other cell lines, including (Human lung cancer cell line A549, gastric cancer cell line MGC80-3, liver cancer cell line SK-HEP-1, colon cancer cell line RKO). The results demonstrated that PKM2 knockdown selectively and significantly decreased PK activity (Fig. 1 *F* and *G*), but did not significantly affect the activities of other glycolytic enzymes (Table S1). Similar to HeLa cells, PKM2 KD did not significantly affect the rate of glycolysis (glucose consumption and lactate production) in these cells (Fig. 1 *H* and *I*).

The above results demonstrated that PKM2 KD caused a large drop in PK concentration, but did not cause a significant change in the rate of glycolysis, indicating that there is no dose-effect relationship between the glycolysis rate and the concentration of PKM2, suggesting that the large change in PKM2 concentration did not affect the actual activity of PK in the glycolysis pathway. Moreover, the PKM2 KO experiments demonstrated that even in the absence of PKM2, the residual PK activity still could maintain the glycolytic rate. The results are consistent with previous studies reported by us (18) and others (20). However, this raises another question: how the actual activity of PK is maintained in the glycolytic pathway.

The reciprocal relationship between the concentration of PK and the concentration of its substrate PEP

Although PKM2 is the dominant isoform in cancer cells, other PK isotypes (PKL, PKR, and PKM1) also exist (12, 23). We did Western blotting to detect the expression of these isoenzymes. The band of PKM2 was dominant, the band of PKLR (PKL + PKR, note that the antibody used cannot distinguish PKL from PKR) was appreciable, while the band of PKM1 was faint (Fig. S1).

Given that pyruvate kinase (PK) in these cancer cell lines comprises PKM1, PKM2, PKL, and PKR, the activity of PK within the glycolytic pathway is contributed by all four isoenzymes. The actual activity of PK in the glycolytic pathway is determined not only by the concentrations of PK but also by its substrate PEP. Although PKM2 KD or KO decreased the concentrations of PK, it may induce an increase in the concentrations of PEP and ADP, the substrates of PK. The increased concentration of PEP and ADP may maintain the actual activity of PK by counteracting the reduced concentration of PK. The concentrations of PEP in HeLa-NC and HeLa-siPKM2 were 0.07 and 0.21 mM, respectively, while the ADP concentrations in HeLa-NC and HeLa-siPKM2 were comparable without significant difference (Fig. 2*A*), hence it is the concentrations of PEP but not ADP that affect the PK activity. According to the kinetics of PK *versus* PEP (Fig. 2*B*), the slope of the kinetic curve in the range of PEP concentration between 0.07 and 0.21 mM was steep, thus the increased concentration of PEP in HeLa-siPKM2 may markedly increase the catalytic velocity of PK and may compensate the decreased concentration of PK. To consolidate the argument, we did an enzyme assay to measure the activity of PK, in which the concentration of PEP was set at the cellular concentration of PEP, *i.e.*, the activity of PK in the cell lysate was assayed at a PEP concentration of 0.07 and 0.21 mM for HeLa-NC and HeLa-siPKM2, respectively. Under such conditions, the activity of PK in the cell lysate prepared from HeLa-siPKM2 was even significantly higher than that from HeLa-NC (Fig. 2*C*).

PKM2 KO significantly elevated the concentration of PEP but not ADP (Fig. 2*D*). When measuring the activity of PK in the cell lysate prepared from HeLa-PKM2-KO and HeLa-px459 using their cellular concentration of PEP (0.25 mM, and 0.08 mM, respectively, for HeLa-PKM2-KO and HeLa-px459), there was no significant difference from each other. (Fig. 2*E*).

Then, we did the same experiments on four other cancer cell lines, PKM2 KD significantly increased the concentrations of PEP but not ADP (Fig. 2, F–I), and it did not significantly reduce the activity of PK when assayed at their cellular concentration of PEP (Fig. 2, *J*–*M*).

Collectively, PKM2 KD or KO induced an increase in PEP concentrations in the tested cancer cells, and the increased concentration of PEP could compensate for the reduced concentration of PK. The next question is: since the actual activity of PK in the glycolytic pathway is determined by both concentrations of PK and PEP, when PK is perturbed, how is the concentration of PEP regulated in the glycolytic pathway.

The built-in thermodynamic properties in the glycolytic pathway and the auto-equilibration of the intermediate concentrations in the glycolytic pathway

The built-in thermodynamic properties in the glycolytic pathway refer to the reaction quotients (Qs) and ΔGs of the

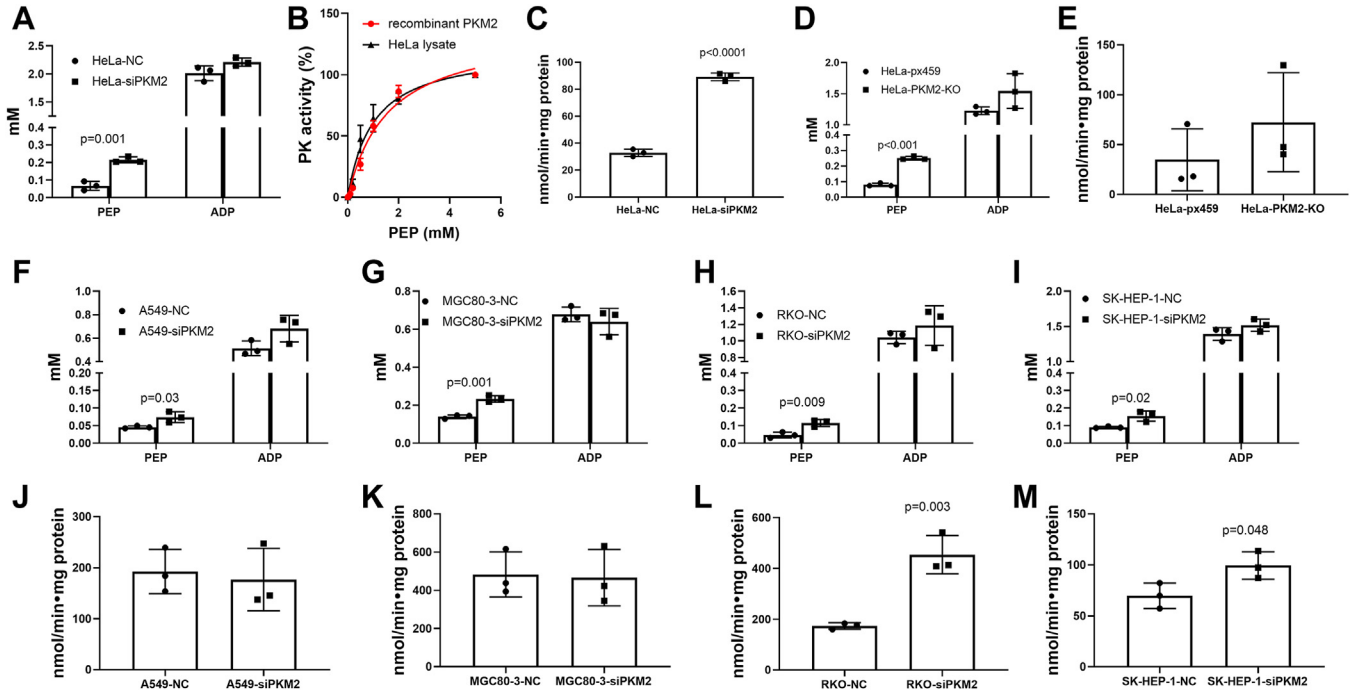

Figure 2. PKM2 KD- or KO-induced elevation of PEP concentration compensate the decreased concentrations of PK. *A*, PEP and ADP concentrations in HeLa-NC and HeLa-siPKM2 cells. *B*, kinetics of recombinant PKM2 and PK from HeLa lysate *versus* PEP concentrations. *C*, Actual PK activity was measured at cellular PEP concentrations for HeLa-NC lysate (0.07 mM) and HeLa-siPKM2 lysate (0.21 mM) cells. *D*, PEP and ADP concentrations in HeLa-px459 and HeLa-PKM2-KO cells. *E*, Actual PK activity was measured at cellular PEP concentrations for HeLa-px459 lysate (0.07 mM) and HeLa-PKM2-KO lysate (0.25 mM). *F–I*, PEP and ADP concentrations in control and PKM2 knockdown cells of A549, MGC80-3, RKO, and SK-HEP-1. *J–M*, PK activity in the cell lysates measured at their corresponding cellular PEP concentrations (PEP concentrations for A549 with or without PKM2 KD, 0.07 and 0.05 mM; PEP concentrations for MGC80-3-C with or without KD, 0.23 and 0.14 mM; PEP concentrations for RKO with or without PKM2 KD, 0.11 and 0.05 mM; PEP concentrations for SK-HEP-1 with or without PKM2 KD, 0.15 and 0.09 mM). Data represent the mean ± SD of three independent experiments with each experiment performed in triplicates.

reactions along the glycolytic pathway. We measured the concentrations of the glycolytic intermediates in HeLa-siPKM2 and HeLa-NC cells. The concentrations of PEP, 2-PG, 3-PG, GA3P, DHAP, and FBP were significantly higher in HeLa-siPKM2 than HeLa-NC (Fig. 3*A*, the upper left panel). These glycolytic intermediates were located in the segment between PK and PFK1 (Fig. 3*A*, the lower panel). The concentrations of other intermediates including G6P, F6P, pyruvate, NAD, NADH, ADP, and ATP were not significantly changed. This pattern of the concentration change of the glycolytic intermediates was also seen in HeLa-PKM2-KO (Fig. 3*A*, the upper right panel) and other PKM2 KD cells, including A549-siPKM2, MGC80-3-siPKM2, RKO-siPKM2, and SK-HEP-1-siPKM2 (Fig. S2*A*).

Figure 3, *B* and *C* are the Q values and ΔG values of the reactions along the glycolytic pathway in HeLa-NC & HeLa-siPKM2 and HeLa-px459 & HeLa-PKM2-KO, where Qs are calculated using the measured data of the intermediate concentrations (Fig. 3*A*) and the ΔGs are calculated by inserting Q values into the equation of Gibbs free energy.

The thermodynamic properties in the glycolytic pathway are similar between HeLa-NC and HeLa-siPKM2. In the pathway, three reactions catalyzed by HK2, PFK1, and PK are highly exogonic, providing the driving force for glucose converting to pyruvate in the pathway (Fig. 3*B*, right panel). The ΔG of the reaction catalyzed by LDH is about −7.8 kJ/mol, which is thermodynamically favorable for converting pyruvate + NADH to lactate + NAD. The other reactions in the pathway are at a thermodynamically near-equilibrium state, hence these reactions are responsible for maintaining the concentrations of intermediates, meaning that the concentrations of the glycolytic intermediates in HeLa-NC and HeLa-siPKM2 are in fact determined by the thermodynamic properties in the glycolytic pathway.

Despite the similarity, there are differences in thermodynamics in the glycolytic pathway between HeLa-NC and HeLa-siPKM2. In HeLa-siPKM2, the ΔG of the reaction catalyzed by PK is −28.6 ± 0.4 kJ/mol, in contrast to −25.1 ± 1.4 kJ/mol in HeLa-NC, meaning that this reaction is even more exogonic in HeLa-siPKM2 than in HeLa-NC cells. On the other hand, the ΔG of the reaction catalyzed by PFK1 in HeLa-siPKM2 cells is −10.8 ± 0.9 kJ/mol, in contrast to −13.3 ± 1.0 kJ/mol in HeLa-NC, meaning that this reaction in HeLa-siPKM2 cells is less exogonic than that in HeLa-NC. The differences could readily explain that more free energy is accumulated in the segment between PFK1 and PK in the glycolytic pathway in HeLa-siPKM2 cells, manifested by the leveled-up Gibbs free energy between this segment (Fig. 3*B*, right panel), and more free energy in this segment is equivalent to more intermediate accumulated in this segment. This is the thermodynamic basis underlying the proportional increase of the concentrations of FBP, DHAP, GA3P, 3-PG, 2-PG, and PEP in the glycolytic pathway in HeLa-siPKM2.

Based on the built-in thermodynamic properties in the glycolytic pathway, we could make the following inferences.

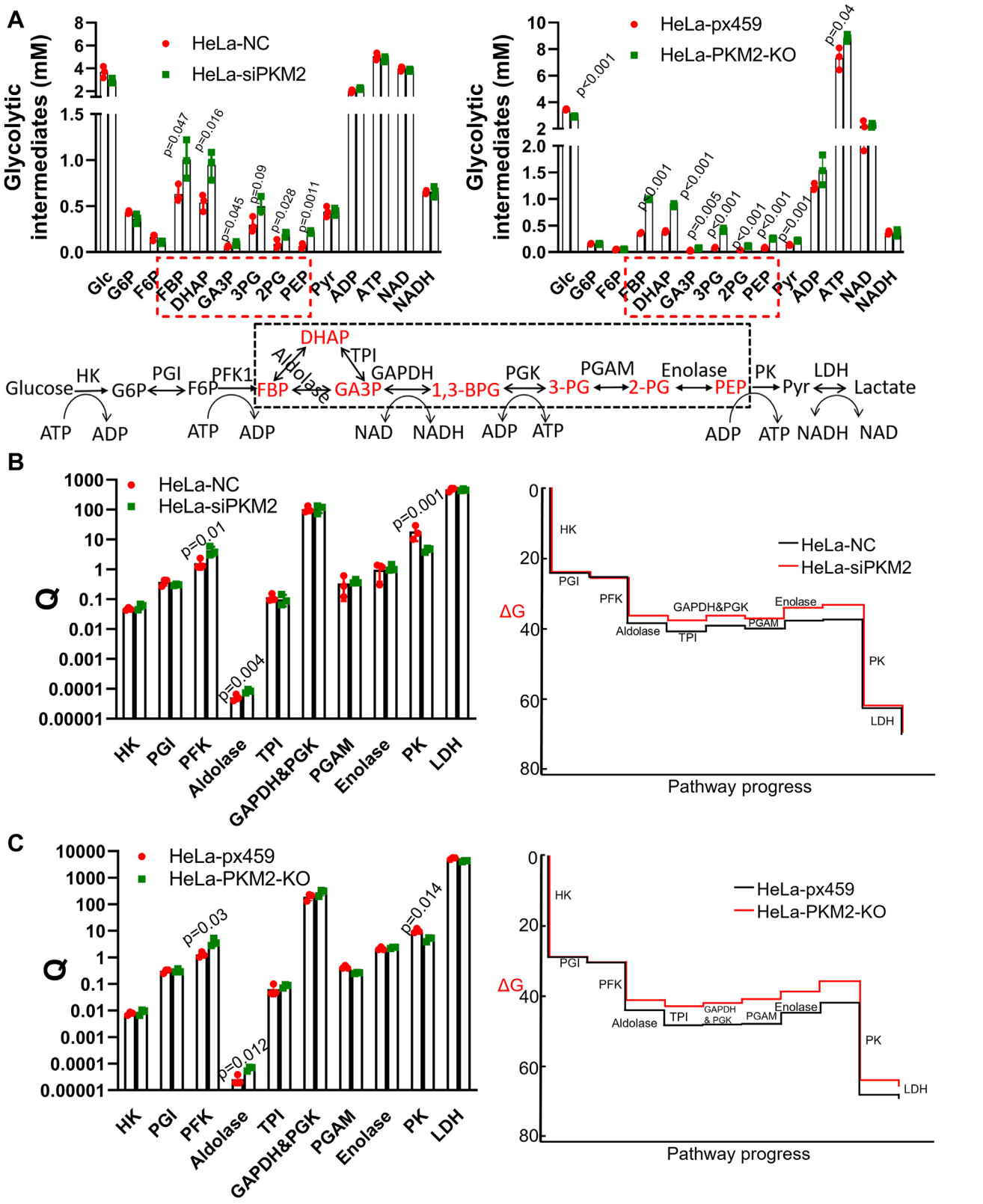

Figure 3. The relationship between PKM2 KD- or KO-induced concentration changes in the intermediates and the thermodynamic properties in the glycolytic pathway. *A*, *upper* panel, intracellular concentrations of glycolytic intermediates in HeLa-NC & HeLa-siPKM2 and HeLa-px459 & HeLa-PKM2-KO (data from Table S2). Lower panel, Schematic glycolysis pathway (words in red denote the intermediates, whose concentrations are significantly increased after PKM2 KD or KO). *B* and C, Q and ΔGs of the reactions along the glycolysis in cells with or without PKM2 KD or KO (data from Table S3). Data are mean ± SD, n = 3. Results were confirmed by two independent experiments.

First, in HeLa-siPKM2, the concentration of PKM2 is substantially lower than in HeLa-NC, resulting in a decrease in its catalytic rate. On the other hand, since the upstream rate of glycolysis is not inhibited, the concentration of PEP (the substrate of PKM2) would increase, which in turn increases the catalytic rate of PKM2 and eventually restore its catalytic rate. The immediate upstream of PKM2 is a reaction catalyzed by enolase, which catalyzes the conversion between 2-PG and PEP. Because enolase-catalyzed reaction in the glycolytic pathway is at a near-equilibrium state, an increase in the concentration of PEP would lead to a proportional increase in the concentration of 2-PG. By the same analogy, the upstream of enolase are sequentially PGAM, PGK1, GAPDH, TPI, and aldolase. Because these reactions in the glycolytic pathway are all in a near-equilibrium state, the concentrations of 3-PG, GA3P, DHAP, and FBP were also increased proportionally, eventually reaching a kinetic and thermodynamic steady state. Thus, the built-in thermodynamic properties in the glycolytic pathway are responsible for equilibrating the intermediate concentrations and autoregulating a reciprocal relationship between the concentration of PKM2 and the concentration of PEP: when the concentration of PKM2 reduces, the concentration of PEP increases, and *vice versa*, enabling a stable activity of PKM2 in the glycolysis.

Second, then why the concentrations of G6P and F6P remains unchanged. Some previous reports demonstrated that PKM2 inhibition can significantly increase the concentrations of G6P and F6P in the glycolytic pathway in cancer cells (8, 17). In principle, this is unlikely to happen in HeLa cells, because the ΔG of PFK1-catalyzed reaction in HeLa-siPKM2 is still −10.8 kJ/mol, which is far from thermodynamic equilibrium. In other words, if PKM2 KD could cause an increase in [G6P] and [F6P], according to the Gibbs Free Energy equation, if the intracellular concentrations of ATP, ADP, and F6P were maintained at cellular levels (Table S2), FBP concentration would reach as high as 130 mM (*e.g.*, in HeLa cells); likewise, if the intracellular concentrations of FBP, ADP, and F6P were maintained at cellular levels (Table S2), ATP concentration would be as low as 0.025 mM (*e.g.*, in HeLa cells). This explains that PKM2 KD-induced distribution of free energy is constrained in the segment of the glycolytic pathway between PK and PFK1.

Finally, when PK resumes its catalytic rate, pyruvate concentration in HeLa-siPKM2 and HeLa-NC should be the same, and indeed there were no significant differences in the measured values (Fig. 3*A* upper left panel, Table S2).

The abovementioned findings and analysis were reproduced in HeLa PKM2 KO model (Fig. 3, *A* and *C*) and PKM2 KD models using other cancer cells (Fig. S2). The ΔGs of the reactions in this segment were at a near thermodynamic equilibrium state, similar to control cells (Fig. S2*C*). Thus, the thermodynamics in the glycolytic pathway responding to PKM2 KD or KO is similar.

Collectively, we deciphered the thermodynamic basis for the glycolytic pathway in cancer cells with or without PKM2 KD or KO and interpreted the interrelationship between PKM2, the intermediates, and the thermodynamic properties in the glycolytic pathway. This could rationally explain why PKM2 KD or KO did not significantly or only marginally alter the glycolytic rate.

Moderate increase of glucose carbon to serine synthesis pathway in HeLa-siPKM2

The above results demonstrated that in PKM2 KD or KO cells, the concentrations of the intermediates (including 3-PG) in the segment between PFK1 and PK in the glycolysis pathway increases. As 3-PG is the precursor of serine, glucose carbon to serine synthesis may increase. We traced [$^{13}C_6$]Glc to serine. The m0 species of serine and m0 glycine are provided by the culture medium, and the m3 serine and m2 glycine are generated from [$^{13}C_6$]Glc through 3-PG. Knockdown of PKM2 did not affect the glycolysis rate within 9 h (Fig. 4*A*), consistent with the results in Figure 1*B*. HeLa-siPKM2 showed a higher rate of both m0 serine consumption and m3 serine generation than HeLa-NC (Fig. 4*B*). Serine could be converted to glycine *via* serine hydroxymethyl transferase in cells. In consistency with serine metabolism, HeLa-siPKM2 showed a higher rate of both m0 glycine consumption and m2 glycine generation than HeLa-NC (Fig. 4*C*). In another of our studies (unpublished data), we quantified the rate of glucose through 3-PG to serine, which is about 1/80 of that of glucose to lactate, so the increased rate of glucose to serine induced by PKM2 KD is not high enough to significantly affect the rate from glucose to lactate.

Marginally increased growth rate of HeLa-siPKM2

It is well recognized that the rapid proliferation of cancer cells is supported by the high rate of aerobic glycolysis (24). Previous reports demonstrated that PKM2 KD could affect cancer cell growth *via* regulating glycolytic rate (7, 17, 25) as well as glycolytic intermediate 3-PG to serine synthesis pathway (SSP), in other words, these studies strongly suggest a cause-effect relationship between PKM2, glycolysis, and cell growth. In our study, PKM2 KD did not significantly inhibit glycolysis but significantly enhanced 3-PG to serine synthesis. As serine De Novo synthesis occupies an important position in cancer metabolism (26), we sought to confirm if PKM2 KD-induced enhancement of SSP exerts an effect on cancer cell growth. HeLa-siPKM2 harbored a marginally but significantly higher percentage of S phase cells, a lower percentage of G0&G1 phase cells, and a comparable percentage of G2/M phase cells, in comparison to HeLa-NC (Fig. 4, *D* and *E*). HeLa-siPKM2 also showed a marginally but not significantly higher growth than HeLa-NC (Fig. 4*F*), accompanied by a marginally higher glucose consumption and lactate generation (Fig. 4*G*).

Dominant allosteric regulation of PKM2 by FBP in enzyme assay

Several models have been proposed to interpret how PKM2 switches between low- and high-activity forms. FBP, a glycolytic intermediate, is a potent allosteric activator of PKM2 (10, 11). When FBP accumulates, PKM2 tetramerizes and this is a

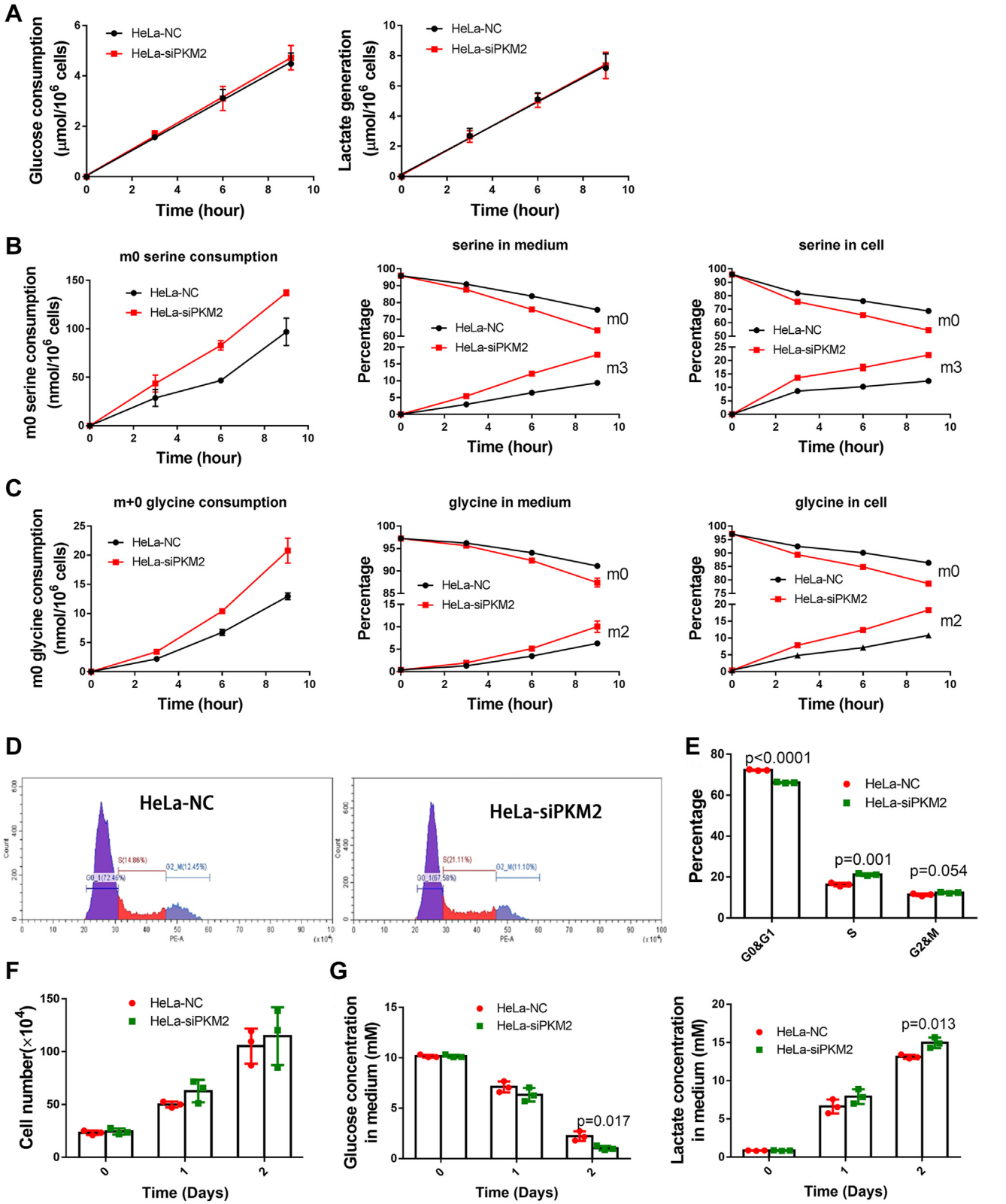

Figure 4. PKM2 knockdown moderately increases glucose carbon to serine synthesis pathway and marginally increases cell growth rate. *A*, glucose consumption and lactate generation by HeLa-NC and HeLa-siPKM2 cells. *B*, serine consumption and serine synthesis by HeLa-NC and HeLa-siPKM2. *Left* panel, consumption of m0 serine provided by the culture medium; middle panel, percentage of m0 and m3 serine in medium; right panel, percentage of m0 and m3 serine in cells. *C*, glycine consumption and glycine synthesis by HeLa-NC and HeLa-siPKM2 cells. *Left* panel, consumption of m0 glycine provided by the culture medium; the *middle* panel, percentage of m0 and m2 glycine in medium; the *right* panel, percentage of m0 and m2 glycine in cells. *D*, representative flow cytometry images of cell cycle analysis of HeLa-NC and HeLa-siPKM2 cells. *E*, Cell cycle distribution of HeLa-NC and HeLa-siPKM2 cells. *F*, cell number of HeLa-NC and HeLa-siPKM2 cells at 0, 1, and 2 days after the transfected cells were seeded to new plates. *G*, glucose and lactate concentrations in culture medium of HeLa-NC and HeLa-siPKM2 cells. Data represent the mean ± SD of three independent experiments with each experiment performed in triplicates.

high-activity form, and it depletes upstream intermediates including FBP, favoring energy production; when FBP is depleted, PKM2 is dissociated to dimer, which is a low-activity form, and then upstream glycolytic intermediates including FBP are accumulating, favoring intermediates for biosynthesis purpose. Serine and PKM2 also form a positive feedback loop to regulate glycolysis. Serine is an allosteric activator of PKM2 (13): when serine concentration is low, PKM2 activity decreases, leading to the accumulation of upstream intermediates including 3-PG and enhancing serine synthesis; when serine is sufficient, PKM2 activity increases, decreasing the rate of 3-PG converting to serine while increasing glycolytic rate to lactate. In addition to allosteric activators, numerous allosteric inhibitors of PKM2 were defined, including alanine, phenylalanine, proline, tryptophan, valine, etc (14, 15, 27). In theory, the activity of PKM2 in cells is constantly co-regulated by all these allosteric inhibitors and activators.

In cancer cells, PKM2 is co-regulated by numerous allosteric effectors. As the concentrations of these allosteric effectors could change dynamically, it is generally conceived that PKM2 is dynamically equilibrated between different states, for example, T and R state, tetramer and dimer, enabling highly dynamic change of PKM2 activity (7, 13–16, 28, 29). Nevertheless, PK activity exposed to the mixture of allosteric activators and inhibitors at their cellular concentrations is unknown. In order to investigate the combined effect of these allosteric effectors on PKM2 activity in different cancer cells, we should answer the following questions:

First, the effect of these allosteric regulators on PKM2 in different cancer cells may be different, *e.g.*, PKM2 could be modified (*e.g.*, phosphorylation, acetylation, *etc.*) (17, 30) differently in different cells, and the different modifications may change the kinetic properties of PKM2. Indeed, the sensitivity of PK from different cancer cells to allosteric regulators differed from each other, as manifested by the IC_{50}s (alanine, phenylalanine, proline, tryptophan, valine) or AC_{50} (FBP and serine) (Fig. S3, Table S4), *e.g.*, at saturating concentrations of FBP or serine, the magnitude of activity change of PKM2 could differ significantly between different cells (Fig. S3, *B* and *C*).

Second, the concentrations of these allosteric regulators in different cells may differ from each other. We show that the concentrations of alanine, phenylalanine, proline, tryptophan, valine, FBP, and serine were significantly different from each other (Table S5). Among the five allosteric inhibitors, the concentration of alanine was the highest on average and the concentration of tryptophan was the lowest on average. The concentration of alanine ranged between 1.36 ± 0.50 mM (HeLa) and 5.78 ± 1.57 mM (RKO). According to the curves of PK activity *versus* alanine (Fig. S3), we could estimate PK activity exposed to such alanine concentration in cells. In the five cancer cells, alanine alone could inhibit PK by 98% (SK-HEP-1) to 89% (MGC80–-3) (Table S5). In the same way, we could estimate PK activity according to the cellular concentration of each allosteric inhibitor or activator (Table S5).

Third, the combined effect of these allosteric regulators on PKM2 activity in these cells is unknown. We assayed PK activity in the cell lysate in the presence of these allosteric regulators at their cellular concentrations (Table S5). For example, in HeLa cells, the concentrations of alanine, phenylalanine, proline, tryptophan, valine, serine, and FBP were 1.36 ± 0.50, 0.29 ± 0.04, 1.39 ± 0.15, 0.12 ± 0.01, 0.70 ± 0.21, 1.39 ± 0.34, and 0.38 ± 0.04 mM, respectively, so when determining PK activity in the HeLa cell lysate, the assay mixture contained these regulators at the above-indicated concentrations, and so forth for other cells (Table S5). Unless otherwise stated, the cellular concentrations of FBP, serine, and amino acid mixture in the subsequent figures and text are the same as above. PK activity was enhanced by serine and FBP in the absence of an allosteric inhibitor mixture (alanine, phenylalanine, proline, tryptophan, and valine; Fig. 5*A*), which is termed AIM in the manuscript. The potency of serine and FBP to activate PK activity was comparable. When PK activity was assayed with AIM and without serine or FBP, the residual PK activities were in the range between (16 ± 5.5) % (RKO) and (3.0 ± 1.9) % (A549) (Fig. 5*A*). The addition of serine did not significantly reverse the inhibition. The addition of FBP not only completely reversed the inhibition but also activated PK activity to the level without AIM. The effect of FBP plus serine on PK inhibition by AIM was the same as that of FBP alone (Fig. 5*A*).

Further, we sought to determine the AC_{50}^{FBP} and AC_{Max}^{FBP} for PK with or without saturating concentration of AIM. The concentration of each allosteric inhibitor in this assay is about 10 folds of the IC_{50} (2.0 mM alanine, 0.7 mM phenylalanine, 2 mM proline, 1 mM tryptophan and 1.0 mM valine for cell lysate; 2.0 mM alanine, 0.7 mM phenylalanine, 5 mM proline, 2.5 mM tryptophan, and 3.0 mM valine for pure recombinant PKM2). According to the curves (Fig. 5*B*), without AIM, the AC_{50}^{FBP} is 28.9 ± 21.0 nM (SK-HEP-1) to 67.2 ± 32.4 nM (RKO), the minimum concentration for maximal activation is 216.4 ± 52.8 nM (HeLa) to 279.0 ± 143.1 nM (A549) (Table S6). With AIM, 349.6 ± 31.2 nM (MGC80–3) to 585.2 ± 99.0 nM (HeLa) FBP could completely reverse the inhibition of PK by the AIM (Fig. 5*B*, Table S6), AC_{50}^{FBP} were 682.1 ± 126.2 nM (A549) to 1066.1 ± 393.6 nM (RKO), AC_{Max}^{FBP} was 1258.9 ± 245.4 nM (A459) to 2293.7 ± 503.7 nM (HeLa). Note that the maximal activity of PK activated by FBP with or without AIM were comparable without statistical significance (Fig. 5*B*).

Based on the above results, because intracellular FBP is between 0.21 mM (RKO)-0.80 mM (SK-HEP-1) in the tested cancer cells (Table S2), which are all much higher than AC_{Max}^{FBP}, we speculate that FBP plays a dominant role in the allosteric regulation of PKM2 in cells.

Estimation of PK activity in the glycolysis pathway by taking allostery into consideration

It is noted in Figure 2 that the activities of PK in the cell lysates (HeLa-siPKM2, RKO-siPKM2, and SK-HEP-1-siPKM2) by taking cellular PEP concentration into consideration were significantly higher than those of controls. This is probably because PKM2, PKL, and PKR are all allosteric enzymes

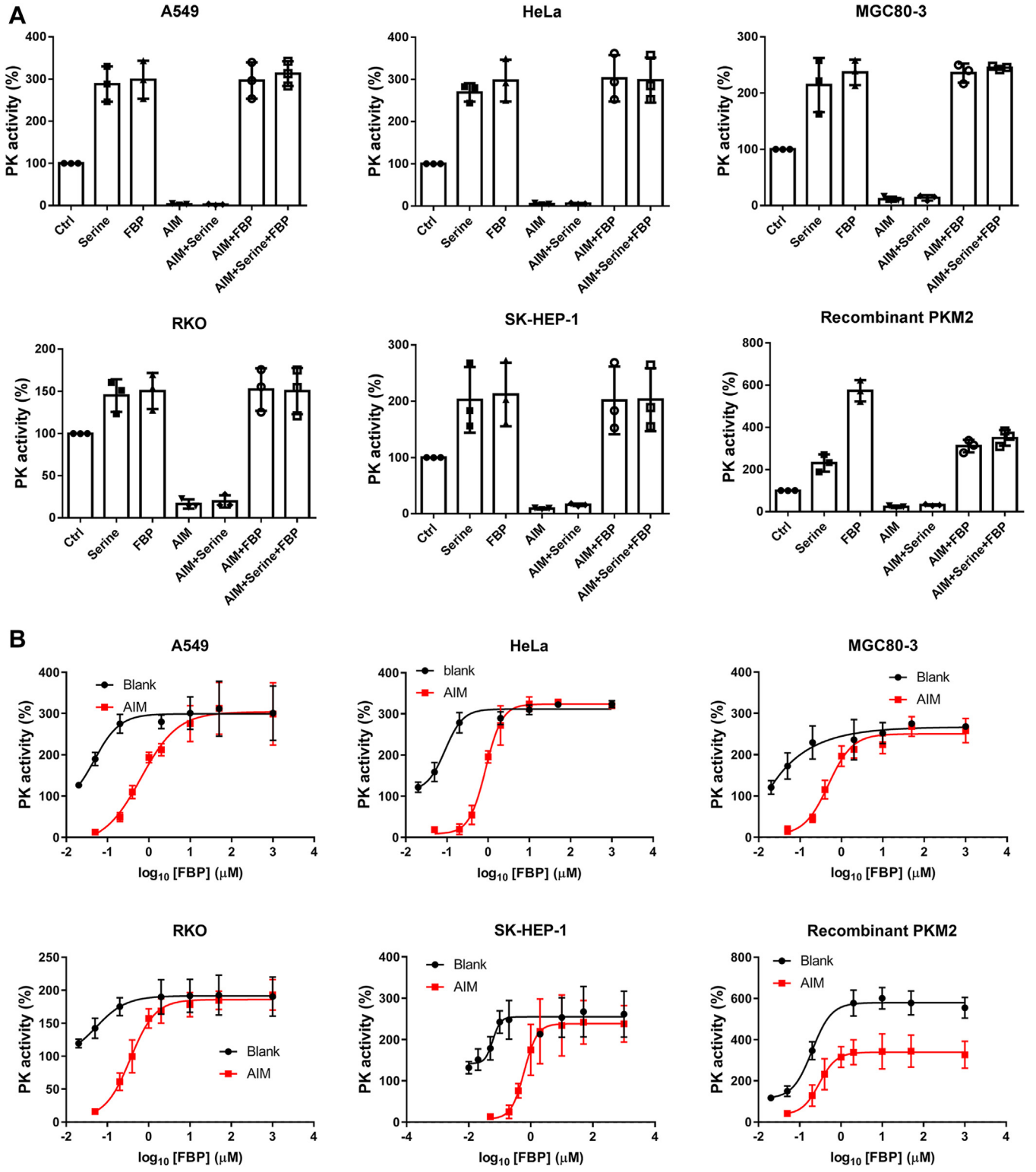

Figure 5. The dominating role of FBP in the allosteric regulation PK. *A*, The dominating role of FBP in the allosteric regulation of cell lysate PK or recombinant PKM2. For measuring the activity of PK in the cell lysate, cellular concentrations of FBP, serine, and AIM were used (see Table S5 for cellular concentrations of these regulators). For measuring the activity of pure recombinant PKM2, AIM used were 2.0 mM alanine, 2.0 mM phenylalanine, 5.0 mM proline, 2.5 mM tryptophan, and 3.0 mM valine; Serine and FBP concentrations used were 5 mM and 0.1 mM, respectively. The substrate concentrations were 2 mM ADP and 0.2 mM PEP. PK activities measured without allosteric regulators were used as controls. *B*, kinetic profiles of pyruvate kinase activities at different FBP concentrations with or without AIM. For cell lysate, AIM consisted of 2.0 mM alanine, 0.7 mM phenylalanine, 2 mM proline, 1 mM tryptophan and 1.0 mM valine. For pure recombinant PKM2, AIM used were 2.0 mM alanine, 2.0 mM phenylalanine, 5.0 mM proline, 2.5 mM tryptophan and 3.0 mM valine. The substrate concentrations were 2 mM ADP and 0.2 mM PEP. PK activities measured without FBP or AIM were used as control (100%). Data represent the mean ± SD of three independent experiments with each experiment performed in triplicates.

(31, 32) and the allostery should be also taken into consideration.

To address this issue, we first measured the PK activity in the cell lysate prepared from cancer cells with or without PKM2 KD or KO under conditions as described in Figure 5*A*. Despite the markedly loss of the total activity (Fig. 6*A*), when converting to percentage-wise, the allostery of PK in cell lysate prepared from cells with or without KD or KO were virtually the same (Fig. 6*B*), supporting that the remaining PK activity are mostly allosteric enzymes, consistent with the Western blot results (Fig. S1). Then we assayed the PK activity in the cell lysate prepared from the cells with or without PKM2 KD/KO in the condition described in the Figure 2 with allosteric regulators at their cellular concentrations. Under such conditions, the PK activity in the cell lysate prepared from cells with or without PKM2 KD/KO was not significantly different from each other (Fig. 6*C*). The data in Figure 6, in line with those in Figure 2, support that by taking cellular concentrations of PK, PEP, and allosteric regulators (FBP and AIM) into consideration, the actual activities of PK activity in the glycolytic pathway with or without PKM2 KD or KO are comparable.

The interrelationship between PK, intermediates, and thermodynamic properties in the glycolytic pathway in cell-free glycolysis system

In cells, glycolysis is connected to its subsidiary pathways and it is integrated into a whole network of metabolism, hence perturbations of PKM2 may exert a complex effect on metabolism, which then could feedback to affect PKM2 and glycolysis. To observe a pure effect of PKM2 perturbation on glycolysis, we need an isolated system for this purpose. We used a cell-free glycolysis, which could be considered an isolated glycolysis system (18, 21, 22).

The total activity of PK in the HeLa-siPKM2 lysate was about 30% of that in the HeLa-NC cell lysate (Fig. 1*A*). HeLa-NC or HeLa-siPKM2 cell lysate was added into a reaction buffer containing all the substrates and cofactors to initiate glycolysis. The glucose consumption rate and lactate generation rate were comparable between the two groups (Fig. S4*A*). The concentrations of FBP, DHAP, GA3P, 3-PG, 2-PG, and PEP were significantly higher in HeLa-siPKM2 lysate group than in HeLa-NC lysate group (Fig. S4*B*). In the HeLa-siPKM2 lysate group, the ΔG of PFK1-catalyzed reaction was less negative (less exogonic) and the ΔG of PK-catalyzed reaction was more negative (more exogonic) than those in the HeLa-NC lysate group (Fig. S4*C*), the other reactions in the glycolytic pathway were all at near equilibrium state, indicating that the concentrations of the intermediates were well equilibrated by the thermodynamic properties in the glycolytic pathway in both groups (Fig. S4*C*). The above thermodynamic states of the reactions along the pathway explain why the concentrations of FBP, DHAP, GA3P, 3-PG, 2-PG, and PEP were proportionally higher in the HeLa-siPKM2 lysate group than those in the HeLa-NC lysate group.

According to the concentrations of PEP and FBP in the cell-free glycolysis system (Fig. S4*B*), we can measure the actual PK activity. The assay condition for PK actual activity in the cell-free glycolysis system using HeLa-NC cell lysate, the PEP concentration and FBP concentrations were 8.2 μM and 34.9 μM, respectively, while the assay condition for actual PK activity in the cell-free glycolysis system using HeLa-siPKM2 cell lysate, the PEP and FBP concentrations were 16.0 μM and 38.8 μM, respectively. Under such conditions, the actual PK activities between HeLa-NC and HeLa siPKM2 were not significantly different (Fig. S4*D*). This thermodynamic equilibration of the intermediates concentration well interpreted the reciprocal relationship between the concentration of PK and the concentration of PEP which stabilizes the activity of PKM2 in the glycolytic pathway (Fig. S4*D*), even the total PK activity between the two groups differed by 3.3 folds, *i.e.*, the increased concentration of PEP could compensate the decreased concentration of PK in the cell-free glycolysis system.

Using the same procedure, we repeated the experiment of cell-free glycolysis by using cell lysate of HeLa-px459 and HeLa-PKM2-KO and obtained similar results. Although the total activity of PK in the HeLa-PKM2-KO lysate was about 18% of that in the HeLa-px459 cell lysate (Fig. 1*D*), the glucose consumption rate and lactate generation rate were only about 10% lower in the HeLa-PKM2-KO group (Fig. S4*E*). In the PKM2 KO group, the concentrations of FBP, DHAP, GA3P, 3-PG, 2-PG, and PEP were significantly increased (Fig. S4*F*), the ΔG of PFK1-catalyzed reaction was less negative (less exogonic) and the ΔG of PK-catalyzed reaction was more negative (more exogonic) than those in the HeLa-px459 lysate group (Fig. S4*G*), the other reactions in the glycolytic pathway were all at near equilibrium state, indicating that the concentrations of the intermediates were well equilibrated by the thermodynamic properties in the glycolytic pathway in both groups (Fig. S4*G*). The PK actual activity in the cell-free glycolysis between the two groups was not significantly different from each other (Fig. S4*H*).

Collectively, the results based on the cell-free glycolysis fully support the conclusion that the auto-equilibration of the intermediate concentrations by the thermodynamic properties in the glycolytic pathway can compensate for the decreased concentration of PKM2 or PK.

Dominant allosteric regulation of PKM2 in the glycolytic pathway by FBP

Although FBP is dominant over multiple allosteric effectors in enzyme assays (Fig. 5), it is unknown if FBP also plays a dominant role in the regulation of PKM2 in the glycolysis pathway, as the regulation of PKM2 in enzyme assay and in the glycolytic pathway are two different questions. To investigate this issue, we made the following inferences. In the presence of multiple allosteric effectors, if FBP plays a dominant role in the allosteric regulation of PKM2 in the glycolysis, there would be no significant changes of the ΔGs of reactions catalyzed by PKM2 and PFK1, and neither proportional change of the concentrations of glycolytic intermediates including FBP, DHAP, GA3P, 3-PG, 2-PG, and PEP. Otherwise, there would be significant changes in the ΔGs of reactions catalyzed by

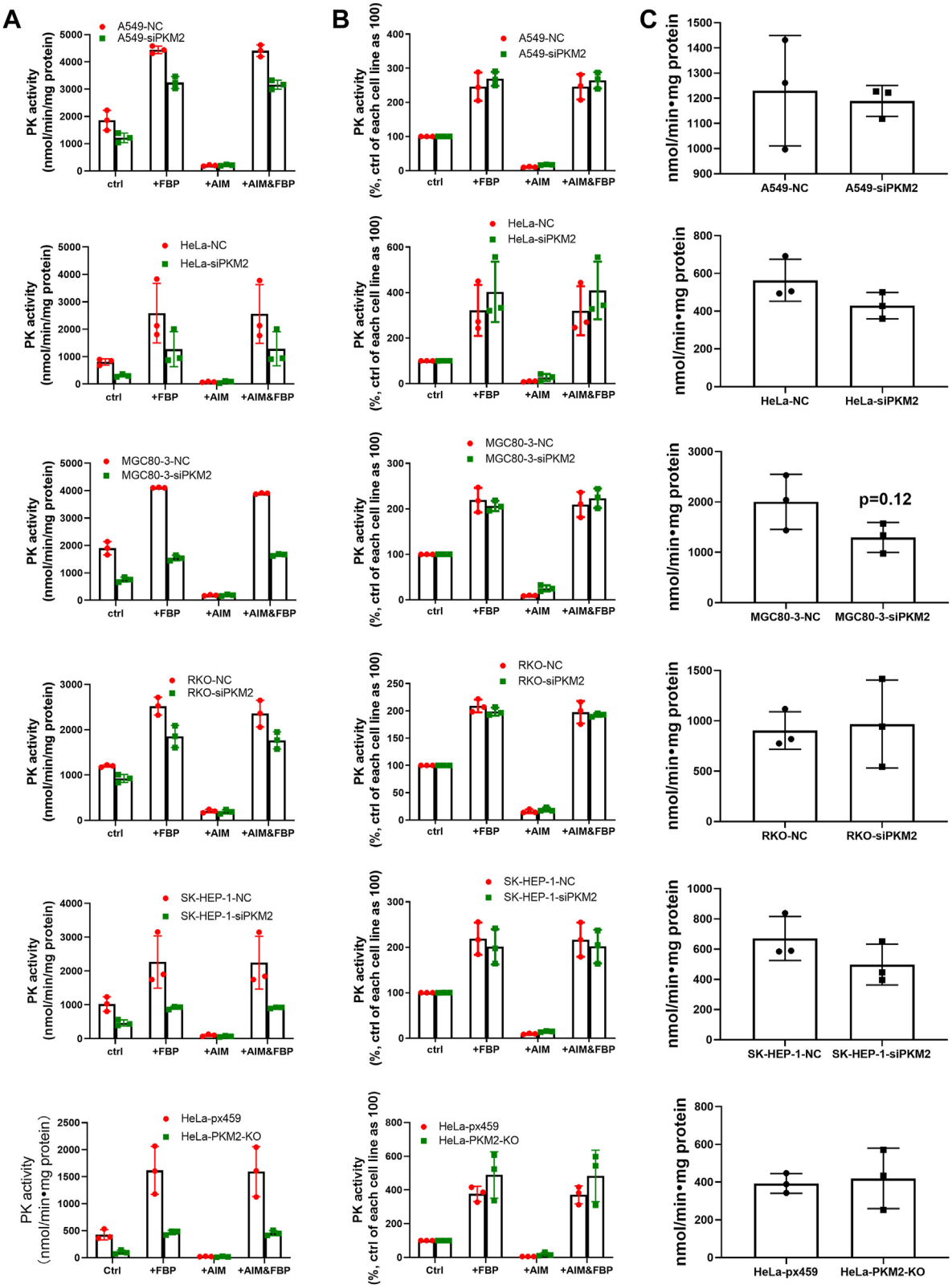

Figure 6. The remaining PK in PKM2-KD cells is allosterically regulated. *A*, PK activity assayed with or without cellular concentrations of FBP, AIM or FBP & AIM. Cell lysates of control, PKM2 KD or KO cells were prepared for PK activity measurement under the assay condition the same as Figure 5*A*. *B*, conversion of the PK activity (*A*) into a percentage, the ctrls (control cell lysate and PKM2 KD cell lysate or PKM2 KO cell lystate in the absence of allosteric regulators were set at 100%). *C*, actual PK activity of the cell lysate under the cellular concentration of PEP, FBP, and AIM. Data represent the mean ± SD of three independent experiments with each experiment performed in triplicates.

PKM2 and PFK1 and there would be proportional changes in the concentrations of glycolytic intermediates including FBP, DHAP, GA3P, 3-PG, 2-PG, and PEP.

We treated HeLa cells with AIM. The cellular concentrations of the alanine, phenylalanine, proline, tryptophan, and valine in the treated cells were increased to 258%, 321%, 368%, 1402%, and 194% relative to control cells (Fig. 7*A*), respectively. The concentration of FBP generated in the glycolytic pathway was around 0.4 mM (Fig. 2*A*), far higher than its A C_{Max}^{FBP} to PKM2 (Table S6). If AIM inhibits PKM2 in the glycolytic pathway, we would observe a significant change of the ΔGs of the reactions catalyzed by PKM2 and PFK1, coupled with a proportional increase of concentrations of FBP, DHAP, GA3P, 3-PG, 2-PG, and PEP. If FBP produced in the glycolytic pathway holds dominant allosteric regulation of PKM2, we would not observe these changes. The results demonstrated that AIM did not significantly alter the concentration of glycolytic intermediates (Fig. 7*B*), the Q values (Fig. 7*C*), nor the ΔG values (Fig. 7*D*) of the reactions along the glycolytic pathway. In addition, AIM did not significantly change glucose consumption or lactate generation (Fig. 7*E*). Therefore, AIM did not significantly inhibit the activity of PKM2 in the glycolytic pathway, and FBP played a dominant role in the allosteric regulation of PKM2 in the glycolytic pathway.

Next, we used cell-free glycolysis assay to further verify whether AIM exerts a significant effect on PKM2 in glycolysis, and whether FBP produced in the glycolysis pathway plays a major allosteric regulation on PKM2 effect. The addition of AIM did not have any significant effect on glycolysis: including glucose consumption rate, lactate production rate (Fig. 7*F*), concentration of glycolytic intermediates (Fig. 7*G*), Qs (Fig. 7*H*), and ΔGs (Fig. 7*I*) for each reaction in the glycolytic pathway. These results further verified that AIM has no significant regulatory effect on PKM2 in the glycolysis pathway. This is because the concentrations of FBP generated in the

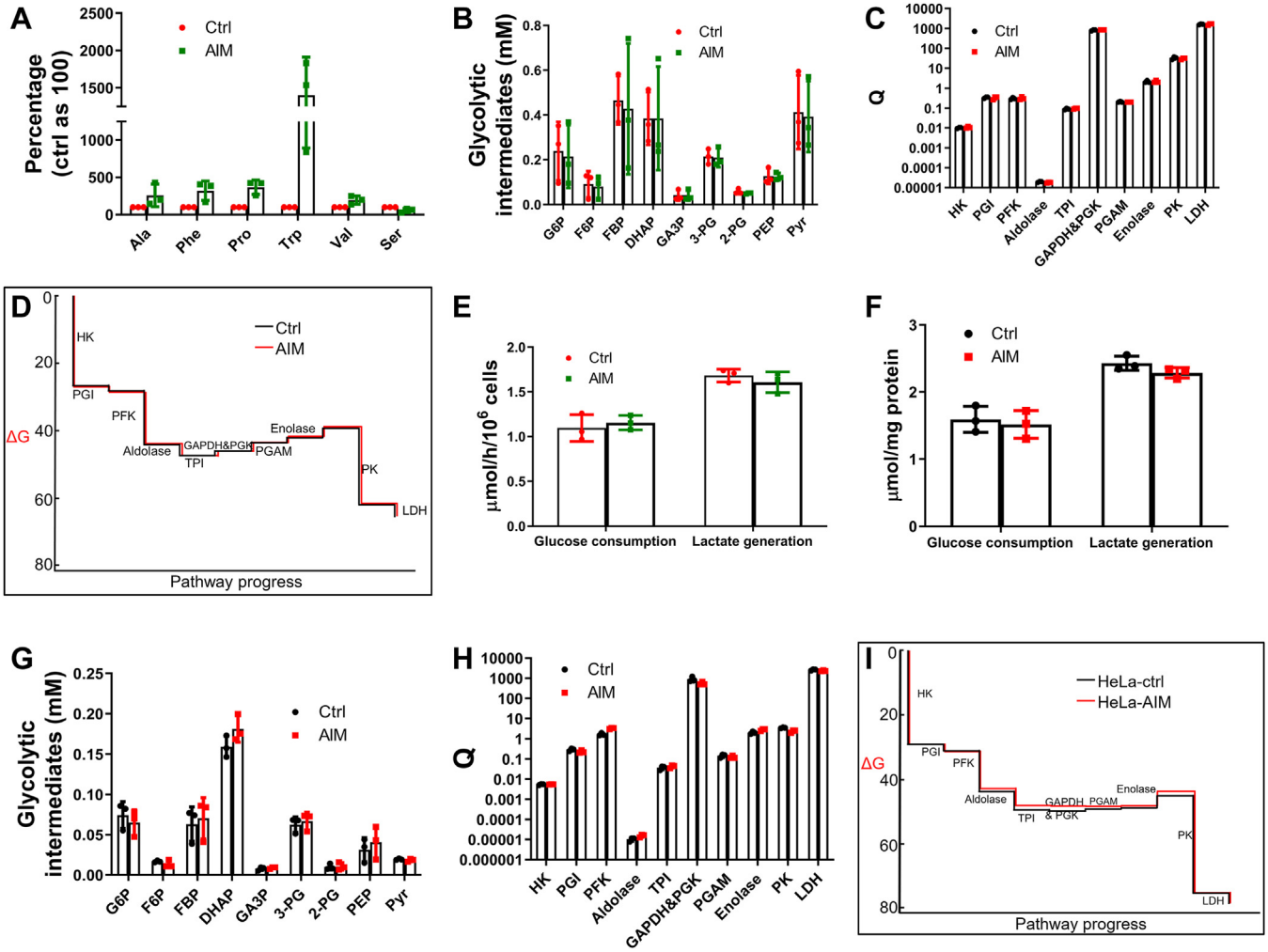

Figure 7. No significant effect of AIM on glycolysis. *A–E*, HeLa cells were cultured in regular RPMI-1640 medium with or without additionally added AIM (2.0 mM alanine, 0.7 mM phenylalanine, 2 mM proline, 1 mM tryptophan, and 1 mM valine) for 5 h. Supernatant and cells were collected and subjected for analysis. *A*, intracellular amino acids. *B*, intracellular glycolytic intermediates. *C* and *D*, Qs and ΔGs of the reactions along the glycolytic pathway (data from Table S9). *E*, Glucose consumption and lactate generation. (*F–I*) Cell-free glycolysis assay using HeLa cell lysate with or without AIM (2.0 mM alanine, 0.7 mM phenylalanine, 2 mM proline, 1 mM tryptophan and 1 mM valine). *F*, glucose consumption and lactate generation. *G*, Glycolytic intermediates. *H* and *I*, Qs and ΔGs of the reactions along the glycolytic pathway (data from Table S9) Data represent the mean ± SD of three independent experiments with each experiment performed in triplicates.

glycolysis flux were about 50 μM (Fig. 7*G*), which is sufficient to dominate the allosteric regulation (Table S6).

Using the same procedure, we checked if serine could affect PKM2 activity in the glycolytic pathway. HeLa cells were treated with 5 mM serine and the cellular serine was increased by 8.3 folds (Fig. 8*A*) relative to control cells, which were about 12 folds higher than AC_{Max}^{serine} toward PKM2. If serine could activate PKM2 in the glycolytic pathway, PFK1-catalyzed reaction would be more exogonic while PKM2-catalyzed reaction less exogonic, leading to a proportional decrease in the concentrations of FBP, DHAP, GA3P, 3-PG, 2-PG, and PEP. If FBP produced in the glycolytic pathway had dominant allosteric regulation of PKM2 in the glycolytic pathway, there would be no significant change of the ΔGs of the reactions

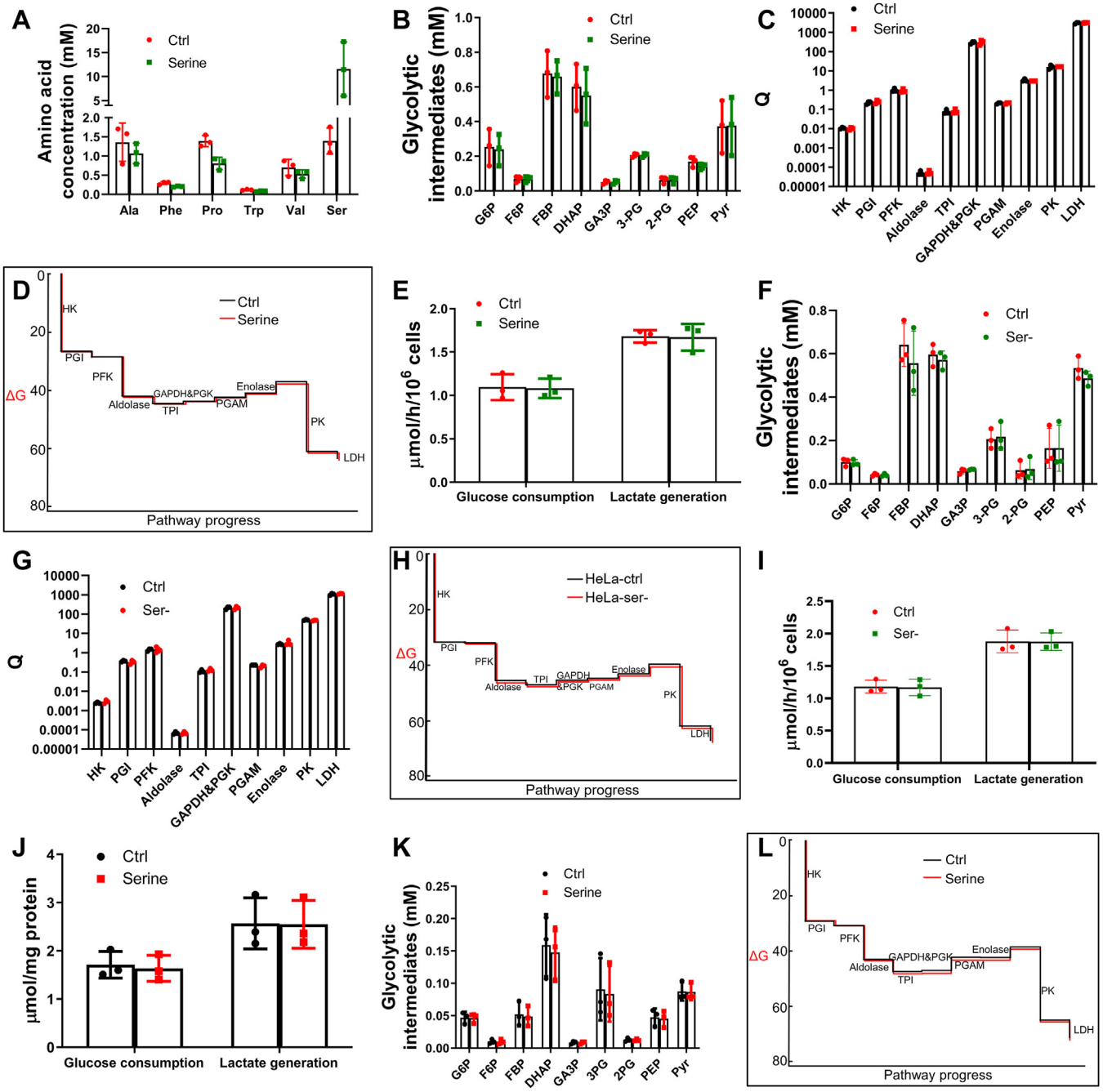

Figure 8. No significant effect of serine on glycolysis. *A–E*, HeLa cells were cultured in RPMI-1640 medium with or without additionally added 5 mM serine for 5 h. Supernatant and cells were collected and subjected for analysis. *A*, intracellular amino acids. *B*, intracellular glycolytic intermediates. *C* and *D*, Qs and ΔGs of the reactions along the glycolytic pathway (data from Table S10). *E*, Glucose consumption and lactate generation. *F–I*, HeLa cells were deprived of serine overnight, then the cells were cultured in fresh culture medium with or without serine for 5 h. Supernatant and cells were collected and subjected for analysis. *F*, Intracellular glycolytic intermediates. *G* and *H*, Qs and ΔGs of the reactions along the glycolytic pathway (data from Table S10). *I*, Glucose consumption and lactate generation. *J–K*, Cell-free glycolysis assay using HeLa cell lysate with or without 5 mM serine. *J*, Glucose consumption and lactate generation. *K*, Glycolytic intermediates. *L*, ΔGs of the reactions along the glycolytic pathway (data from Table S10). Data represent the mean ± SD of three independent experiments with each experiment performed in triplicates.

catalyzed by PKM2 and PFK1, neither significant change of the concentrations of FBP, DHAP, GA3P, 3-PG, 2-PG, and PEP. The results demonstrated that the concentration of glycolytic intermediates (Fig. 8*B*), the Qs (Fig. 8*C*), and ΔGs (Fig. 8*D*) of the reactions along the glycolytic flux were comparable between treated and control cells. Moreover, with or without serine treatment, glucose consumption and lactate generation were also comparable (Fig. 8*E*). Conversely, deprivation of serine did not significantly change the concentration of glycolytic intermediates, the Qs and the ΔGs of the reactions in the glycolytic pathway (Fig. 8, *F–H*), and the glucose consumption and lactate generation (Fig. 8*I*). Using cell-free glycolysis assay, we did not observe serine exert any significant effect on glycolysis, including glycolytic rate (Fig. 8*J*), intermediate concentrations (Fig. 8*K*) and the ΔGs along the glycolytic pathway (Fig. 8*L*). The results confirmed that FBP generated from the glycolytic pathway exerts a dominant allosteric regulation of PKM2 over serine.

We then applied the same principle to check the effect of TEPP-46, a well-defined potent activator of PKM2 with $AC_{90}^{TEPP-46}$ of 0.47 μM (9). First , we tested PK activity in HeLa cell lysate with or without TEPP-46. Without FBP, TEPP-46 markedly enhanced PK activity by about 2.8 folds; with FBP at cellular concentrations (0.4 mM), TEPP-46 did not significantly enhance PK activity (Fig. S5*A*). Second , we used cell-free glycolytic assay to determine the effect of TEPP-46 (1 μM, the saturating concentration for activating PK activity according to Fig. S5*A*) on glycolysis. The results demonstrated that, with or without TEPP-46, the parameters of glycolysis were comparable, including glucose consumption and lactate generation (Fig. S5*B*), the concentrations of the glycolytic intermediates (Fig. S5*C*) , the Qs and the ΔGs of reactions along the glycolytic pathway (Fig. S5, *D* and *E*), indicating that FBP generated from glycolysis is sufficient to exert dominant regulation on PKM2. Finally, we tested the effect of TEPP-46 on cellular glycolytic flux. HeLa cells were treated with or without TEPP-46 (1 μM). The results showed that TEPP-46 exerted no significant effect on glycolytic rate (Fig. S5*F*), nor intermediate concentrations (Fig. S5*G*), nor the Qs (Fig. S5*H*), nor the ΔGs of the reactions along the pathway (Fig. S5*I*). The three levels of experiments confirmed each other that TEPP-46 did not significantly regulate PKM2 in the glycolysis pathway in the presence of FBP and that FBP generated from the glycolytic pathway is sufficient to dominate the allosteric regulation of PKM2.

Discussion

In summary, we have elucidated the interaction between PKM2 and the thermodynamics in the glycolysis pathway. PKM2 KD or KO exerts an effect on thermodynamic properties of the glycolytic pathway, characterized by the reciprocal changes of the ΔGs of the reactions catalyzed by PFK1 and PK. The changes in the ΔGs of the two reactions cause the accumulation of intermediates in the segment between PFK1 and PK. This mechanism maintains the reciprocal relationship between PK concentration and its substrate PEP concentration, by which, PK activity in the glycolytic pathway can be stabilized *via* constant autoregulation, similar to 'feedback' regulation. Although PKM2 is the dominant isoform in cancer cells, other PK isotypes (PKL, PKR, PKM1) also exist (12, 23) (Fig. S1). Thus, the PK activity in these cells is the sum of the activities of four isozymes, *i.e.*, in the glycolytic pathway, the reaction (PEP + ADP + Pi to pyruvate + ATP) is catalyzed by 4 PK isoenzymes. In control cells, PKM2 accounts for most of the PK activity, in PKM2 KD cells, PKM2 activity is reduced and the relative activity of other PK isoenzymes increased, and in PKM2 KO cells, PKM2 is absent, this reaction is catalyzed by other PK isoenzymes. Thus, the thermodynamics of the glycolytic pathway is intrinsically linked to the total concentration of PK, not limited to the concentration of PKM2 alone.

Unlike previously published studies investigating the rate control of glycolysis by PKM2, we took into account the thermodynamic properties of glycolysis. The new perspective reveals that thermodynamic properties serve as systemic regulators of glycolysis that participate in stabilizing the rate of glycolysis in cancer cells and it can effectively counteract perturbations of PKM2, as illustrated in Figure 9. The findings provide fresh insight into the rate control of glycolysis but inevitably lead to conceptual arguments as described below:

First, we introduce new explanations for PKM2 KD/KO-induced changes in the concentrations of glycolytic intermediates, which is different from those in the previous publications (9, 11, 13, 17). The reason for this divergence stems from whether or not to take into account the thermodynamics of glycolysis. In the published literature, since the thermodynamic properties of glycolysis were not counted, the PKM2 inhibition-induced increases in the concentration of upstream intermediates were interpreted as proof of concept that glycolysis was inhibited. However, in essence, the increase of the concentrations of the upstream intermediate (PEP, 2-PG, 3-PG, GA3P, DHAP, FBP) reflects thermodynamic equilibration in the pathway responding to PKM2 depletion. Depletion of PKM2 causes its catalyzed reaction in the pathway more exogonic, leading to the accumulation of upstream intermediates. On the other hand, because the PFK1-catalyzed reaction is far from thermodynamic equilibrium, the increase in the concentration of intermediates is constrained in the segment between PKM2 and PFK1. Because the reactions lying between PFK1 and PKM2 are all in a state of thermodynamic equilibrium, the concentrations of PEP, 2-PG, 3-PG, GA3P, DHAP, and FBP increase proportionally. In the previous reports, PKM2-perturbation could also significantly alter the concentrations of G6P and F6P (8, 17), apparently, the ΔG of PFK1-catalyzed reaction was not taken into consideration.

Second, the above discussion introduces a fresh explanation regarding the relationship between PKM2 or PK, glycolytic rate, and the distribution of glycolytic intermediates to energy and biosynthesis. Most studies reported that the glycolytic rate in cancer cells is sensitive to changes in PKM2 activity. When PKM2 activity fluctuates, the glycolytic rate, the distribution of

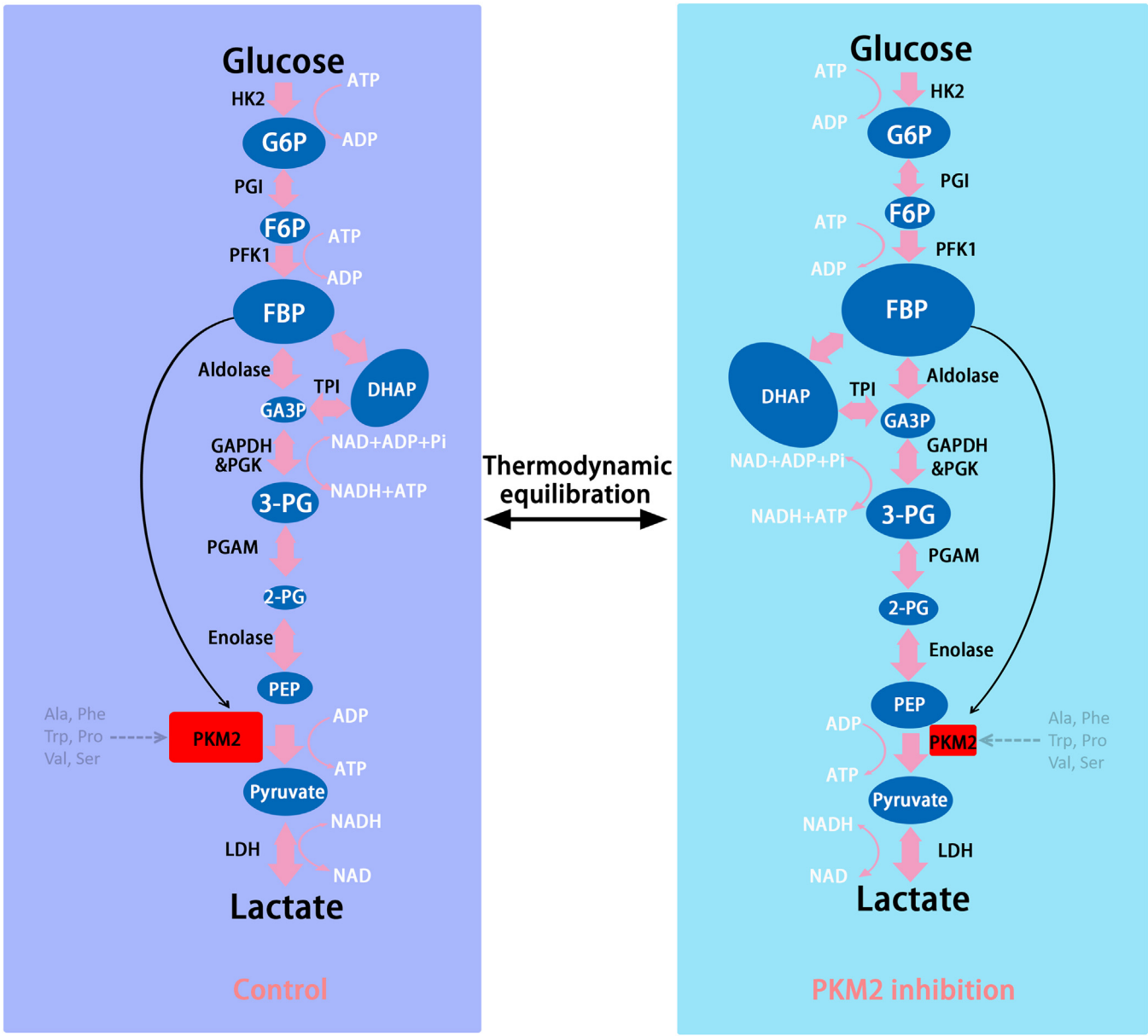

Figure 9. Schematic diagram to demonstrate the autoregulation of PKM2 activity in the glycolytic pathway. PKM2 activity in the glycolytic pathway is stabilized by two mechanisms. First, when PKM2 is inhibited (*e.g.*, PKM2 KD), through the auto-equilibration of the intermediate concentrations by the built-in thermodynamic properties in the glycolytic pathway, the increased concentration of PEP could compensate the reduced concentration of PKM2 (for details, please refers to 'The built-in thermodynamic properties in the glycolytic pathway and the auto-equilibration of the intermediate concentrations in the glycolytic pathway' under the Results Section). Second, FBP generated from glycolysis dominates the allosteric regulation of PKM2, making the enzyme not affected by other allosteric regulators in cells. The sizes of the blue oval (⬭) represent the relative concentrations of intermediates according to the Q values or Δ G values of the reactions along the glycolytic pathway; the size of the rectangle (▭) represents the relative concentrations of PKM2 in control and PKM2 knockdown cells; the pink allow (⇩) represents the rate; the arrow (↘) represents allosteric dominance of PKM2 by FBP over other allosteric effectors (⇢).

glycolytic intermediates to energy and biosynthesis changes accordingly (8, 9, 11, 13, 17). However, there are also reports to the contrary (18–20). Our study pointed out that the activity of PK or PKM2 in the glycolytic pathway in tumor cells is different from its activity in isolation as in enzyme assay. If PK or PKM2 exhibits activity in isolation (such as in enzyme assay), its activity would be linearly related to its concentration. On the other hand, as PKM2 exhibits activity in the glycolytic pathway, its activity is regulated by the built-in thermodynamic properties of the glycolytic system, which has not been recognized in the previous literature. As such, the activity of PKM2 does not have a linear relationship with its concentration, instead, its activity is determined by the reciprocal relationship between its concentration and its substrate concentration, and this reciprocal relationship is maintained by the ΔGs of a series of reactions along the glycolysis, not by PKM2-catalyzed reaction alone. In other words, this reciprocal relationship is autoregulated by the thermodynamic properties

in the glycolytic pathway, through which the activity of PKM2 in the glycolytic pathway is stabilized. Therefore, even after depleting 80% of PKM2 by knockdown, the rate of glycolysis was not significantly affected. When depleting 100% of PKM2 by knockout, the residual PK activity can maintain 90% rate of glycolysis. Overall, it is reasonable to speculate that if PKM2 activity only fluctuates up and down at a baseline, its effects on glycolysis rate and the distribution of glycolytic intermediates to energy and biosynthesis would be minimal.

Finally, there is a concern about the effect of allosteric regulation of PKM2 on glycolysis. Because there are numerous allosteric effectors of PKM2 in cancer cells and the concentrations of these allosteric effectors change dynamically (13–15, 29), it is generally conceived that PKM2 exists in dynamic equilibrium between low- and high-activity form, and this dynamic equilibrium is closely associated with the glycolytic rate and distribution of glucose carbon to biosynthetic and energy purpose. When the allosteric inhibitors are relatively dominant, the activity of PKM2 is low, and the rate of glycolysis decreases, resulting in the accumulation of upstream intermediates, which flux into subsidiary metabolic branches, such as pentose phosphate pathway, serine synthesis pathway, and among others (13, 25). When allosteric activators are relatively dominant, the rate of glycolysis increases, the upstream intermediate concentrations decrease, and glucose carbons flow toward pyruvate and lactate (13, 33). Our study argues with this conception. The concentration of FBP in the glycolysis pathway in cancer cells was at 0.21 to 0.8 mM, and the intracellular FBP concentrations were even higher when PKM2 was genetically depleted. Thus, intracellular FBP is at much higher concentrations than AC_{Max}^{FBP} for PKM2 (Table S6). It should be noted that the concentrations of FBP is maintained by the thermodynamic equilibration in the glycolytic pathway. At such concentrations, FBP dominates the allosteric effect, rendering other allosteric regulators ineffective on PKM2. This dominant allosteric regulation of PKM2 by FBP is validated at three levels, enzyme assays, cell-free glycolysis, and cell glycolysis, which have been explained in detail in the Results section. Our results are also supported by the dissociation constants of allosteric regulators with PKM2. The dissociation constant of PKM2 with FBP is at nM level, whereas the dissociation constants of PKM2 with other allosteric regulators are at μM levels, as listed below: FBP 174 nM, serine 191 μM, phenylalanine 507 μM (34), asparagine 11 ± 2 μM, aspartate 35±7 μM, valine 757 ± 120 μM (35), and cysteine 5.5 μM (27). The dissociation constants are also consistent with the AC and IC data of various allosteric modulators determined in our experiments (Figs. S3 and S4).

The fundamental point in the above debate is whether the thermodynamic properties of glycolysis should be taken into consideration when studying the flux control of glycolysis, and whether the thermodynamic properties of glycolysis play an important role in the flux control of glycolysis in cancer cells. Our study shows that the thermodynamic properties should be regarded as a system property of glycolysis that participates in stabilizing the glycolytic rate in cancer cells.

Experimental procedures

Chemicals and enzymes

Reagents were from Sigma, including ATP (#A3377), ADP (#A5285), NAD (#N0632), NADH (#N8129), NADP (#N8035), NADPH (#N7505), Glucose (#G8270), G6P, (#G7879), F6P (#V900924), GA3P (#G5251), 3-PG (#P8877), 2-PG (#19710), PEP (#P7001), Pyruvate (#V900232), lactic acid (#L1750), HK (#H4502), PGI (#P5381), PFK (#F0137), Aldolase (#A8811), TPI (#T6258), GAPDH (#G2267), PGK (#P7634), Enolase (#E6126), PK (#P7768), LDH (#L2500), G6PDH (#G8404), α-GPDH (#G6751). FBP were purchased from aladdin (China, #F111301).

Cell lines

Human lung cancer cell line A549, cervical cancer cell line HeLa, gastric cancer cell line MGC80-3, liver cancer cell line SK-HEP-1, and colon cancer cell line RKO were obtained from Cell Bank of Type Culture Collection of the Chinese Academy of Science (Shanghai, China) and were all authenticated by DNA fingerprinting and free from *mycoplasma* contamination. One note is that the DNA fingerprinting of MGC80-3 is not separable from that of HeLa cells. However, the morphology of HeLa and MGC80-3 were different from each other and the allostery of PK in the cell lysate from HeLa and MGC80-3 were also different from each other. Cells were cultured in RMPI-1640 medium with 10% FBS and maintained in a humidified incubator at 37 °C with 5% CO_2.

PKM2 knockdown and knockout

For PKM2 KD, 1.6×10^5 cells were seeded into each well of 6-well plates and cultured overnight. Cells were transfected using Lipofectamine 3000 (Thermo Fisher Scientific) according to manufacturer's protocol, with either negative control siRNA (NC) or siPKM2 (Ribobio, China). The siRNA sequences were as follows: siPKM2, sense, GUGGUGAUCUAGGCAUUGAdTdT; antisense, UCAAUGCCUAGAUCACCAC dTdT; NC, sense, UUCUCCGAACGUGUCACGUdTdT; antisense, ACGUGACACGUUCGGAGAA dTdT. 48 h after transfection, cells were washed with PBS and 2 ml fresh complete RMPI-1640 plus 8 mM glucose were added to each well. Then we collected 10 μl media at 4 h and determined glucose & lactate afterwards using the method described by us previously (22). The cells were counted and collected for enzyme activity assay, Western blot, or intracellular intermediates determination. For PKM2 KO, we used the Crispr-Cas9 system according to Feng Zhang's protocol (36) and the procedure was described elsewhere (37). The designed sgRNA sequences were as follows: forward, CACCGATTTGAGGAACTCCGCCGCC; reverse, AAACGGCGGCGGAGTTCCTCA AATC.

PK activity assay

PK activity was assayed under condition as below: cell lysate or purified recombinant PKM2, or PKL was added to a mixture containing 2 mM ADP, 0.2 mM PEP, 0.1 mM NADH, 5 U/ml

LDH in 0.8 ml 37 °C pre-warmed reaction buffer (200 mM HEPES, 0.5 mM EDTA, 100 mM KCl, 5 mM $MgCl_2$, 5 mM Na_2HPO_4, pH 7.4) in a cuvette, to start the assay and absorbance at 340 nm was recorded using a spectrophotometer (DU 700, Beckman Coulter). To determine the allostery of PK, allosteric inhibitors (alanine, phenylalanine, proline, tryptophan, valine) and allosteric activators (FBP, serine) were added into reaction mixtures as described above to desired concentrations, and then cell lysate, or recombinant PKM2 or PKL were added into the reaction mixture to start the reactions. To determine the knockdown efficiency of siRNA, the PEP concentration used was 2 mM.

Purification of human source recombinant PKM2 and PKL

The cDNA of PKM2 and PKL was cloned into pQE-30 (Qiagen) with 6×His tag and expressed in M15 (pREP4) (AngYuBio) as reported by us previously (38). Expression was induced by 0.8 mM Isopropyl-β-D-Thiogalactoside (Beyotime) for 6 h at 32 °C. The cells were collected and sonicated, and lysate was added to a Ni-NTA SefinoseTM Resin column (Sangon Biotech), washed with wash buffer (100 mM Tris-HCl, pH 7.6, 0.5 M NaCl and 20 mM imidazole) and eluted by elution buffer (100 mM Tris-HCl, pH 7.6, 0.5 M NaCl and 250 mM imidazole).

Western blot

Cells were washed with cold PBS, then lysed with M-PER Mammalian Protein Extraction Reagent (Thermo Fisher Scientific) supplemented with cocktail (MedChemExpress) on ice for 30 min. Protein concentration was determined using BCA protein assay kit (Thermo Fisher Scientific). The protein was boiled for 5 min with loading buffer and 20 μg was subjected to 10% SDS-PAGE, transferred to PVDF membrane, and incubated with primary body PKM1 (CST, #7076), PKM2 (HuaBio, #ER1802-70)and PKLR (Proteintech, #22456-1-AP). GAPDH (Proteintech, #60004-1-lg) was used as internal control.

Determination of NAD, NADH, ADP & ATP in cell

Cells in 6-well plates were washed with ice-cold PBS twice, and 0.6 ml 80% (vol/vol) pre-cold (–20 °C) methanol was added per well to extract the intracellular metabolites. Then a scraper was used to collect the cells and the cell debris was discarded by 20,000*g* centrifuge at 4 °C. The supernatant was evaporated by a vacuum centrifugal concentrator and was dissolved in 100 μl water for following UPLC analysis. Waters ACQUITY UPLC system with an ACQUITY UPLC HSS T3 column was used to perform the Liquid Chromatography. Mobile phase A was 20 mM Triethylamine in 99%/1% water/acetonitrile (pH 6.5) and mobile phase B was 100% acetonitrile. The gradient program was as follows: 0 to 9 min, 100% A-90% A; 9 to 10 min, 90% A-0% A; 10 to 11 min, 100% B; 11 to 12 min, 0% A-100% A. 12 to 20 min, 100% A.10 μl sample or standard solution was injected to perform the analysis with a flow rate at 0.3 ml/min. During the performance, the column was kept at 40 °C.

Cell-free glycolysis assay

Previously we had described an *in vitro* cell-free system as a glycolysis model (18, 39). We used the reaction buffer containing 200 mM HEPES, 0.5 mM EDTA, 100 mM KCl, 5 mM $MgCl_2$, 5 mM Na_2HPO_4, 4 mM ADP, 1.5 mM ATP, 5 mM glucose, 0.1 mM NADH, and 2 mM NAD for this glycolysis system. 70 μl lysate (8–10 μg/μl protein) was added to 630 μl reaction buffer, and the mixture was incubated at 37 °C for 30 min. Then we added 600 μl 1 M $HClO_4$ to the mixture to terminate the reaction and later 100 μl 3 M K_2CO_3 was added to neutralize the buffer. The mixture was kept on ice for 20 min further. The supernatant was obtained by 10,000*g* centrifuge at 4 °C and was used for glycolytic intermediates determination.

Determination of glycolytic intermediates, glucose and lactate

Unless otherwise stated, all glycolytic intermediates, glucose, and lactate in cell extracts and cell-free models were measured in this way. For intracellular intermediates, three 10-cm dish cells were washed with PBS, and glycolytic intermediates were extracted using 0.6 ml 1M $HClO_4$. Supernatants were collected by centrifugation and neutralized with K_2CO_3. A second centrifugation was performed to collect the supernatant to measure the intermediates, glucose, and lactate. The detailed methods to determine the glycolytic intermediates, glucose, and lactate were described by us earlier (21, 22).

Determination of intracellular glycolytic intermediates by cycling method

Intracellular glycolytic intermediates (Glucose, G6P, F6P, FBP, DHAP, GA3P, 3-PG, 2-PG, PEP, Pyruvate) in control and PKM2 knockdown cells were determined by cycling method. Negative control or siPKM2 transfected cells were washed by ice-cold PBS twice, and 600 μl 1 M pre-cold $HClO_4$ was added to every five wells of a 6-well plate. Cells were collected by a scraper, incubated on ice for 30 min, and neutralized by 100 μl 3M K_2CO_3. Then supernatant was obtained by 10,000 g centrifuge at 4 °C to perform measurement of the intermediates. The detailed protocol was described by us previously (21, 22).

Calculation of the Gibbs free energy change ΔG of glycolytic reactions

ΔG was calculated as previously reported (22) according to the equation

$$\Delta G = \Delta G'^{0}_{310} + RTnQ$$

where $\Delta G'^{0}_{310}$ is the standard transformed Gibbs free energy at 37 °C and Q was calculated according to intermediate concentrations and was listed in Supplementary Tables. NAD/NADH was set as 78 according to our previously reported

study (18) and [Pi] in the cell was 1.5 mM according to (40). According to ΔG = ΔH-TΔS, since the change of ΔH and ΔS is negligible between 37 °C and 25 °C (41), we deduced the equation to a new form that

$$\Delta G'^{0}_{310} = \frac{310}{298}\Delta G'^{0}_{298} + \left(1 - \frac{310}{298}\right)\Delta H'^{0}_{298}$$

$\Delta G'^{0}_{298}$ and $\Delta H'^{0}_{298}$ are available in references (42–45).

Isotopic lactate determination by LC-MS/MS

[$^{13}C_6$]Glucose was purchased from Sigma. 48 h after transfection, HeLa-NC, HeLa-siPKM2 were washed with PBS twice, and cultured in glucose-free RPMI-1640 supplemented with 10% ultrafiltrated FBS and 6 mM [$^{13}C_6$]glucose for 6 h. Then culture medium was collected and diluted 40 times with 100% acetonitrile and centrifuged at 25,000*g* for 10 min at 4 °C. The supernatant was collected for LS-MS/MS analysis according to methods reported previously by us (46, 47). Briefly, an ACQUITY BEH Amide column was used to perform liquid chromatography, kept at 50 °C during analysis and the injection volume was 7.5 μl. Mobile phase A was 10 mM ammonium acetate in 85% acetonitrile, 15% water, pH 9.0, and mobile phase B was 10 mM ammonium acetate in 50% acetonitrile, 50% water, pH 9.0. The gradient program was as follows: 0 to 0.4 min, 100% A; 0.4 to 2 min, 100–30% A; 2 to 2.5 min, 30–15% A; 2.5 to 3 min, 15% A; 3 to 3.1 min, 15 to 100% A; 3.1 to 7.5 min, 100% A. A 4000 QTRAP mass spectrometer (AB SCIEX) equipped with an ESI ion source (Turbospray) operated in negative ion mode was used for MS detection and the same parameter setting was employed (46).

Amino acid measurement using UPLC

For determination of regular serine, phenylalanine, alanine, valine, proline, and tryptophan in cell, cells in 6-well plates were incubated with or without amino acid mixture (AIM) or serine for 5 h, washed with PBS three times, and intracellular intermediates were extracted by adding 80% pre-cold methanol. Cells were collected by a scraper and 20,000*g* centrifuge at 4 °C was performed and the supernatant was evaporated by a vacuum centrifugal concentrator and was dissolved in 100 μl water. 10 μl dissolved metabolites or amino acid standard was mixed with 20 μl AQC (#ab145409, abcam, amino acid derivatization agent) and 120 μl borate buffer, incubate in 60 °C for 20 min and the AQC derivatized samples were subjected to Liquid Chromatography analysis using Waters Acquity UPLC system with an AccQ-Tag Ultra RP Column. The mobile phase A was 25 mM ammonia formate with 1% acetonitrile, pH 3.05 and mobile phase B was 100% acetonitrile. The gradient program was as follows: 0 to 0.54 min, 99.9% A, 0.1% B; 0.54 to 5.74 min, 99.9% A-90.9% A; 5.74 to 7.74 min, 90.9% A- 78.8% A; 7.74 to 8.04 min, 78.8% A-40.4% A; 8.04 to 8.64 min, 40.4% A. 8.64 to 8.73 min, 40.4% A-99.9% A; 8.73 to 9.5 min, 99.9% A. 1 μl sample or standard solution was injected to perform the analysis with a flow rate at 0.7 ml/min. During the performance, the column was kept at 55 °C.

For determination of isotopic serine and glycine, after 48-h transfection, cells were cultured with glucose-free RMPI 1640 medium supplemented with 10% FBS and 6 mM [$^{13}C_6$]glucose for 3, 6 and 9 h. Medium at 0, 3, 6, 9 h were collected. Meanwhile, cells at 0, 3, 6, 9 h were washed with PBS three times, and intracellular amino acid were extracted and samples were prepared as above mentioned for LC-MS/MS measurement. The Liquid Chromatography conditions were the same as regular amino acids determination, while the following parameters were optimized and used for MASS analysis: 40 psi curtain gas, medium collision gas, 5500V ionspray voltage, temperature of the ion source 500 °C, 40 psi ion source gas1 and 40 psi ion source gas2.

Determination of glycolytic enzyme activity

We determined glycolytic enzyme activity at saturating substrate concentration according to previously reported methods (48) with some modifications. Briefly, 0.8 ml reaction buffer was added to the cuvette, and substrates were added as below. The reaction was started by adding cell lysate and mixed, and then absorbance at 340 nm was recorded using a spectrophotometer (DU 700, Beckman Coulter).

HK: 0.2 mM NADP, 2 mM ATP, 10 mM glucose, 1 U/ml G6PDH, 30 μg protein of lysate;

PGI: 2 mM F6P, 0.2 mM NADP, 1 U/ml G6PDH, 5 μg protein of lysate;

PFK: 0.1 mM ADP, 2 mM ATP, 2 mM F6P, 1 U/ml Aldolase, 0.1 mM NADH, 1 U/ml α-GPDH, 10 μg protein of lysate;

Aldolase: 0.1 mM NADH, 1.5 mM FBP, 1 U/ml α-GPDH, 15 μg protein of lysate;

TPI: 2 mM GA3P, 0.1 mM NADH, 1 U/ml α-GPDH, 1 μg protein of lysate;

GAPDH: 2 mM NAD, 2 mM GA3P, 4 μg protein of lysate;

PGK: 2 mM ATP, 2 mM 3-PG, 0.1 mM NADH, 1 U/ml GAPDH, 5 μg protein of lysate;

PGAM: 2 mM ADP, 1 mM 3-PG, 1 U/ml Enolase, 0.1 mM NADH, 1 U/ml PK, 1 U/ml LDH, 10 μg protein of lysate;

Enolase: 2 mM ADP, 1 mM 2-PG, 1 U/ml PK, 0.1 mM NADH, 1 U/ml LDH, 10 μg protein of lysate;

LDH: 0.1 mM NADH, 2 mM pyruvate, 2 μg protein of lysate.

Cell cycle

Cell cycle assay was performed using a Cell cycle staining Kit (# 70-CCS012, MultiSciences, China) according to the manufacturer's protocol. Briefly, HeLa cells were transfected with NC or siPKM2 for 48 h, trypsinized, and seeded to a new 6-well plate overnight, then collected and subjected to flow cytometer analysis.

Statistical analysis

All experiments were repeated at least 3 times, and all data were analyzed using GraphPad Prism7. For comparisons of two groups, two-tailed Student's *t* test was performed.

Data availability

All data are in the article.

Supporting information—This article contains supporting information.

Acknowledgment—We thank Dr Guo-Hua Fong (University of Connecticut School of Medicine, USA) for constructive comments of our work and critical readings of our manuscript.

Author contributions—X. H. conceptualization; X. H. data curation; X. H., C. J., W. H., and Y. W. formal analysis; X. H. funding acquisition; X. H., W. H., Y. W., and S. Z. investigation; X. H., C. J., W. H., and H. W. methodology; X. H. and H. W. supervision; X. H. and C. J. validation; X. H. writing–original draft; X. H., C. J., W. H., and M. Y. writing–review & editing; C. J. investigation, C. J. data curation.

Funding and additional information—This work has been supported in part by China Natural Science Foundation projects (82073038, 81772947), a key project (2018C03009) funded by Zhejiang Provincial Department of Sciences and Technologies, the Fundamental Research Funds for the Central Universities (2017XZZX001-01, 2019FZJD009, 226-2024-00062), and the National Ministry of Education, China, to X.H.

Conflict of interest—The authors declare no conflicts of interest with the contents of this article.

Abbreviations—The abbreviations used are: ΔG, Gibbs free energy; 2-PG, 2-phosphoglycerate; 3-PG, 3-phosphoglycerate; AIM, allosteric inhibitor mixture; Ala, Alanine; F6P, fructose 6-phosphate; FBP, fructose 1,6-bisphosphate; FBS, fetal bovine serum; G6P, glucose 6-phosphate; G6PDH, glucose-6-phosphate dehydrogenase; GA3P, glyceraldehyde 3-phosphate; GAPDH, glyceraldehyde 3-phosphate dehydrogenase; Glc, glucose; HK, hexokinase; KD, knockdown; KO, knockout; LDH, lactate dehydrogenase; MTS, methanethiosulfonate; NC, negative control; PEP, phosphoenolpyruvate; PES, phenazine ethosulfate; PFK, phosphofructokinase; PGI, phosphohexose isomerase; PGK, phosphoglycerate kinase; Phe, phenylalanine; PK, pyruvate kinase; Pro, proline; Pyr, pyruvate; Q, reaction quotient; Ser, serine; TPI, triose phosphate isomerase; Trp, tryptophan; UPLC, ultra performance liquid chromatography; Val, valine; [x], the concentration of x, *e.g.*, [PK] refers the concentration of PK.

References

1. Warburg, O. (1956) On the origin of cancer cells. *Science* **123**, 309–314
2. Hay, N. (2016) Reprogramming glucose metabolism in cancer: can it be exploited for cancer therapy? *Nat. Rev. Cancer* **16**, 635–649
3. Gatenby, R. A., and Gillies, R. J. (2004) Why do cancers have high aerobic glycolysis? *Nat. Rev. Cancer* **4**, 891–899
4. Vander Heiden, M. G., Cantley, L. C., and Thompson, C. B. (2009) Understanding the Warburg effect: the metabolic requirements of cell proliferation. *Science* **324**, 1029–1033
5. Altenberg, B., and Greulich, K. O. (2004) Genes of glycolysis are ubiquitously overexpressed in 24 cancer classes. *Genomics* **84**, 1014–1020
6. Lunt, S. Y., Muralidhar, V., Hosios, A. M., Israelsen, W. J., Gui, D. Y., Newhouse, L., *et al.* (2015) Pyruvate kinase isoform expression alters nucleotide synthesis to impact cell proliferation. *Mol. Cell* **57**, 95–107
7. Christofk, H. R., Vander Heiden, M. G., Harris, M. H., Ramanathan, A., Gerszten, R. E., Wei, R., *et al.* (2008) The M2 splice isoform of pyruvate kinase is important for cancer metabolism and tumour growth. *Nature* **452**, 230–233
8. Anastasiou, D., Poulogiannis, G., Asara, J. M., Boxer, M. B., Jiang, J. K., Shen, M., *et al.* (2011) Inhibition of pyruvate kinase M2 by reactive oxygen species contributes to cellular antioxidant responses. *Science* **334**, 1278–1283
9. Anastasiou, D., Yu, Y., Israelsen, W. J., Jiang, J. K., Boxer, M. B., Hong, B. S., *et al.* (2012) Pyruvate kinase M2 activators promote tetramer formation and suppress tumorigenesis. *Nat. Chem. Biol.* **8**, 839–847
10. Dombrauckas, J. D., Santarsiero, B. D., and Mesecar, A. D. (2005) Structural basis for tumor pyruvate kinase M2 allosteric regulation and catalysis. *Biochemistry* **44**, 9417–9429
11. Zwerschke, W., Mazurek, S., Massimi, P., Banks, L., Eigenbrodt, E., and Jansen-Durr, P. (1999) Modulation of type M2 pyruvate kinase activity by the human papillomavirus type 16 E7 oncoprotein. *Proc. Natl. Acad. Sci. U. S. A.* **96**, 1291–1296
12. Prakasam, G., Singh, R. K., Iqbal, M. A., Saini, S. K., Tiku, A. B., and Bamezai, R. N. K. (2017) Pyruvate kinase M knockdown-induced signaling via AMP-activated protein kinase promotes mitochondrial biogenesis, autophagy, and cancer cell survival. *J. Biol. Chem.* **292**, 15561–15576
13. Chaneton, B., Hillmann, P., Zheng, L., Martin, A. C. L., Maddocks, O. D. K., Chokkathukalam, A., *et al.* (2012) Serine is a natural ligand and allosteric activator of pyruvate kinase M2. *Nature* **491**, 458–462
14. Morgan, H. P., O'Reilly, F. J., Wear, M. A., O'Neill, J. R., Fothergill-Gilmore, L. A., Hupp, T., *et al.* (2013) M2 pyruvate kinase provides a mechanism for nutrient sensing and regulation of cell proliferation. *Proc. Natl. Acad. Sci. U. S. A.* **110**, 5881–5886
15. Yuan, M., McNae, I. W., Chen, Y., Blackburn, E. A., Wear, M. A., Michels, P. A. M., *et al.* (2018) An allostatic mechanism for M2 pyruvate kinase as an amino-acid sensor. *Biochem. J.* **475**, 1821–1837
16. Christofk, H. R., Vander Heiden, M. G., Wu, N., Asara, J. M., and Cantley, L. C. (2008) Pyruvate kinase M2 is a phosphotyrosine-binding protein. *Nature* **452**, 181–186
17. Lv, L., Li, D., Zhao, D., Lin, R., Chu, Y., Zhang, H., *et al.* (2011) Acetylation targets the M2 isoform of pyruvate kinase for degradation through chaperone-mediated autophagy and promotes tumor growth. *Mol. Cell* **42**, 719–730
18. Xie, J., Dai, C., and Hu, X. (2016) Evidence that does not support pyruvate kinase M2 (PKM2)-catalyzed reaction as a rate-limiting step in cancer cell glycolysis. *J. Biol. Chem.* **291**, 8987–8999
19. Liberti, M. V., Dai, Z., Wardell, S. E., Baccile, J. A., Liu, X., Gao, X., *et al.* (2017) A Predictive model for selective targeting of the warburg effect through GAPDH inhibition with a natural product. *Cell Metab.* **26**, 648–659.e648
20. Tanner, L. B., Goglia, A. G., Wei, M. H., Sehgal, T., Parsons, L. R., Park, J. O., *et al.* (2018) Four key steps control glycolytic flux in mammalian cells. *Cell Syst.* **7**, 49–62.e48
21. Zhu, X., Jin, C., Pan, Q., and Hu, X. (2021) Determining the quantitative relationship between glycolysis and GAPDH in cancer cells exhibiting the Warburg effect. *J. Biol. Chem.* **296**, 100369
22. Jin, C., Zhu, X., Wu, H., Wang, Y., and Hu, X. (2020) Perturbation of phosphoglycerate kinase 1 (PGK1) only marginally affects glycolysis in cancer cells. *J. Biol. Chem.* **295**, 6425–6446
23. Yang, Y., Zhu, G., Dong, B., Piao, J., Chen, L., and Lin, Z. (2019) The NQO1/PKLR axis promotes lymph node metastasis and breast cancer progression by modulating glycolytic reprogramming. *Cancer Lett.* **453**, 170–183
24. Liberti, M. V., and Locasale, J. W. (2016) The warburg effect: how does it benefit cancer cells? *Trends Biochem. Sci.* **41**, 211–218
25. Ye, J., Mancuso, A., Tong, X., Ward, P. S., Fan, J., Rabinowitz, J. D., *et al.* (2012) Pyruvate kinase M2 promotes de novo serine synthesis to sustain mTORC1 activity and cell proliferation. *Proc. Natl. Acad. Sci. U. S. A.* **109**, 6904–6909
26. Ducker, G. S., and Rabinowitz, J. D. (2017) One-carbon metabolism in health and disease. *Cell Metab.* **25**, 27–42

27. Srivastava, D., Nandi, S., and Dey, M. (2019) Mechanistic and structural insights into cysteine-mediated inhibition of pyruvate kinase muscle isoform 2. *Biochemistry* **58**, 3669–3682
28. Israelsen, W. J., Dayton, T. L., Davidson, S. M., Fiske, B. P., Hosios, A. M., Bellinger, G., *et al.* (2013) PKM2 isoform-specific deletion reveals a differential requirement for pyruvate kinase in tumor cells. *Cell* **155**, 397–409
29. Keller, K. E., Doctor, Z. M., Dwyer, Z. W., and Lee, Y. S. (2014) SAICAR induces protein kinase activity of PKM2 that is necessary for sustained proliferative signaling of cancer cells. *Mol. Cell* **53**, 700–709
30. Hitosugi, T., Kang, S., Vander Heiden, M. G., Chung, T. W., Elf, S., Lythgoe, K., *et al.* (2009) Tyrosine phosphorylation inhibits PKM2 to promote the Warburg effect and tumor growth. *Sci. Signal.* **2**, ra73
31. Llorente, P., Marco, R., and Sols, A. (1970) Regulation of liver pyruvate kinase and the phosphoenolpyruvate crossroads. *Eur. J. Biochem.* **13**, 45–54
32. Yamada, K., and Noguchi, T. (1999) Nutrient and hormonal regulation of pyruvate kinase gene expression. *Biochem. J.* **337**, 1–11
33. Keller, K. E., Tan, I. S., and Lee, Y. S. (2012) SAICAR stimulates pyruvate kinase isoform M2 and promotes cancer cell survival in glucose-limited conditions. *Science* **338**, 1069–1072
34. Macpherson, J. A., Theisen, A., Masino, L., Fets, L., Driscoll, P. C., Encheva, V., *et al.* (2019) Functional cross-talk between allosteric effects of activating and inhibiting ligands underlies PKM2 regulation. *Elife* **8**, e45068
35. Nandi, S., and Dey, M. (2020) Biochemical and structural insights into how amino acids regulate pyruvate kinase muscle isoform 2. *J. Biol. Chem.* **295**, 5390–5403
36. Ran, F. A., Hsu, P. D., Wright, J., Agarwala, V., Scott, D. A., and Zhang, F. (2013) Genome engineering using the CRISPR-Cas9 system. *Nat. Protoc.* **8**, 2281–2308
37. Ying, M., You, D., Zhu, X., Cai, L., Zeng, S., and Hu, X. (2021) Lactate and glutamine support NADPH generation in cancer cells under glucose deprived conditions. *Redox Biol.* **46**, 102065
38. Chen, J., Xie, J., Jiang, Z., Wang, B., Wang, Y., and Hu, X. (2011) Shikonin and its analogs inhibit cancer cell glycolysis by targeting tumor pyruvate kinase-M2. *Oncogene* **30**, 4297–4306
39. Xie, J., Wu, H., Dai, C., Pan, Q., Ding, Z., Hu, D., *et al.* (2014) Beyond Warburg effect–dual metabolic nature of cancer cells. *Sci. Rep.* **4**, 4927
40. Giachelli, C. M. (2003) Vascular calcification: in vitro evidence for the role of inorganic phosphate. *J. Am. Soc. Nephrol.* **14**, S300–S304
41. Mendez, E. (2008) Biochemical thermodynamics under near physiological conditions. *Biochem. Mol. Biol. Educ.* **36**, 116–119
42. Alberty, R. A. (2006) Biochemical thermodynamics: applications of Mathematica. *Methods Biochem. Anal.* **48**, 1–458
43. Keleti, T., Foldi, J., Erdei, S., and Tro, T. Q. (1972) Some thermodynamic data on D-glyceraldehyde-3-phosphate dehydrogenase action under optimal conditions. *Biochim. Biophys. Acta* **268**, 285–291
44. Li, X., Wu, F., Qi, F., and Beard, D. A. (2011) A database of thermodynamic properties of the reactions of glycolysis, the tricarboxylic acid cycle, and the pentose phosphate pathway. *Database (Oxford)* **2011**, bar005
45. Varga, A., Szabo, J., Flachner, B., Gugolya, Z., Vonderviszt, F., Zavodszky, P., *et al.* (2009) Thermodynamic analysis of substrate induced domain closure of 3-phosphoglycerate kinase. *FEBS Lett.* **583**, 3660–3664
46. Ying, M., Guo, C., and Hu, X. (2019) The quantitative relationship between isotopic and net contributions of lactate and glucose to the tricarboxylic acid (TCA) cycle. *J. Biol. Chem.* **294**, 9615–9630
47. Zhang, W., Guo, C., Jiang, K., Ying, M., and Hu, X. (2017) Quantification of lactate from various metabolic pathways and quantification issues of lactate isotopologues and isotopmers. *Sci. Rep.* **7**, 8489
48. Passonneau, J. V., and Lowry, O. H. (1993) *Enzymatic Analysis: A Practical Guide*, Humana Press, Totowa, NJ